Interaction Notes

Note 118

September 1972

Small Holes in Cable Shields

R. W. Latham
Northrop Corporate Laboratories
Pasadena, California

Abstract

A discussion of the small hole model for braided cable shields is presented. Four factors upon which the hole polarizabilities depend are examined.

Contents

Figures

Acknowledgement

It's fun to talk to Dr. K. S. H. Lee about the kinds of things discussed in this note. Mr. R. W. Sassman did most of the numerical calculations and Mrs. Georgene Peralta did the typing and drawing.

I. Introduction

The work reported here was motivated by the need to understand braided cable shields. However, many of the results obtained are also applicable to any cable shield that has a single small leak.

The model used to study the braided shield is that of an infinitely thin, perfectly conducting shell with a regular array of small, diamond-shaped holes. Such a model is not new. Vance and Chang [1] have employed a similar model and also have included, in an approximate manner, the effect of the conductivity of the braid wires. There are differences between some of the results here and some of those in reference 1. The reason for these differences is that in the braided shield sections of this note it is assumed that the dominant aperture leakage comes through the holes between intersecting belts of wire, while in reference 1 the aperture leakage was assumed to take place through the holes between individual intersecting wires. But these differences are minor, for either model could be readjusted once the main aperture leakage mechanism has been established.

The purpose of the present note is to use the above model to make a somewhat more detailed analytical study than has been given up to now of the effect of the holes on shielding by braids. A detailed study of the effect of conductivity may be given in a future note.

If one studies a circular, cylindrical, co-axial, braided-shield cable, and one makes the assumption that all wavelengths of interest are long compared to the diameter of the shield, it is possible to set up integro-differential or integral equations for the electric and magnetic potentials in a single aperture by invoking a set of doubly-periodic Green's functions. Such an approach to the problem, if carried through to the numerical computation stage, would necessitate no further approximations in the study of the model. But it would be difficult to develop a feeling for the effect of varying one of the many parameters of the problem by studying the many pages of curves that would be the inevitable result of such a basic, sledgehammer approach. Furthermore, the machine time necessary would be not inconsiderable, and new models would have to be set up to study shielded cables that are not of the simple co-axial type.

The approach taken in this note, and also taken in reference 1, is to try to calculate the effect of a single hole accurately, and then to superpose the effects of all the holes. Of course, this is a rigorous procedure if the effect of each hole were calculated exactly, including its interactions with all the other holes; the approximations enter when the single-hole effect is being calculated. This note extends the work of reference 1 by making possible more accurate estimates of the effect of each hole, although the basic assumption that all wavelengths of interest are much longer than a cable diameter will still be made.

The first step in determining the effect of a single hole in the shield is to derive equivalent voltage and current sources for the hole; these equivalent sources are to be used in conjunction with the transmission-line equations describing cable shielding. It turns out that the equivalent voltage source is proportional to the magnetic dipole moment induced in the hole and that the equivalent current source is proportional to the electric dipole moment induced in the hole. Precise definitions of these induced dipole moments are given in sections II and III. The strength of the magnetic dipole is proportional to the local surface current flowing along the shield, and the strength of the electric dipole is proportional to the local surface charge density on the shield. These are interesting, but intermediate, results. The real problem has been shifted to the computation of the induced dipole moments or, equivalently, the constants of proportionality between the current, linear charge density, and the dipole strengths.

The proportionality constants determining the dipole moments induced in the hole depend on four major factors: (1) the hole shape; (2) the presence of nearby conductors, in particular the proximity of the inner cables; (3) the curvature of the surface at the position of the hole; and (4) the presence of other nearby holes. An estimate of the effect of each of these factors is made in this note, based on accurate solutions to model problems. These model problems are further idealizations of the hole-in-a-shell model. They have been chosen to isolate, as much as possible, one parameter of the overall problem. From a study of these idealized problems, it is hoped that it will become possible to develop some intuition concerning the effects of the various parameters of the real problem, since there are very few parameters

left in each idealized problem. The solutions to the first three idealized problems could also be of interest in the study of nonbraided shields with small isolated holes.

In Section II, a derivation of the equivalent voltage source of an isolated hole in a cable shield is presented. Similar results have been obtained before [2], but the derivation here seems at the same time to be simpler and more general. An example of the general result is given.

In Section III, a derivation of the equivalent current source of an isolated shield hole is presented. Previous results on this type of source [2] don't take quite the same form as they do here, but this is due to differences in the intended use of the expressions. The previous forms of the results were useful for studying the coupling between co-axial cables, while the forms derived in this note are more useful for studying the shielding of cables from external fields. Again the derivation here is rather simple.

Section IV is a brief discussion of the combined effect of the two types of source (voltage and current) when a cable shield with one hole is used to shield a cable from an incident plane wave.

Section V is a detailed discussion of the braided shield model that is used in this note. In particular, the way in which the present work fits into an exact approach described previously [3] is made explicit.

Sections VI through IX are concerned with the detailed solutions and presentations of results of the four idealized problems that have been chosen to study the four factors determining the hole polarizabilities in the braided-shield model. These four factors (hole shape, nearby conductors, surface curvature, and nearby holes) have been mentioned above. Detailed descriptions of the idealized problems chosen to study these factors may be found in the appropriate sections.

Finally, in Section X, another look is given to the braided shield model in the light of the results arrived at in Sections VI through IX.

II. Voltage Source of One Little Hole in a Cable Shield

Figure 1 is a schematic diagram of the situation to be studied. Both the cable and its shield are infinite cylinders, but it is not necessary to assume that they are circular cylinders. In this note it will be assumed that there is only one cable inside the outer shield, although the derivations of the equivalent sources of the hole can readily be generalized if there are several cables inside one shield.

The strength of the equivalent voltage source of the hole is given by $i\omega$ multiplied by the total clockwise difference flux through any infinite strip connecting the inner cable to the shield when a net d.c. current I_s flows along the shield and a net d.c. current I flows along the inner conductor. This follows from previous results [3] if one assumes initially that the shield has a periodic structure with period Δ, and then lets Δ go to infinity. By "difference flux" in the above definition we mean the total flux minus the flux through the same infinite strip if the hole were closed. We will also speak of "difference field" in the following work; this field is the real field minus the field that would exist if the hole were closed. In this section, the boundary-value problem implicit in the above definition of the voltage source will be called the main problem.

We can arrive at an alternative way of calculating the strength of the equivalent voltage source by considering first an auxiliary boundary-value problem — the one where the hole is closed and a current I_o flows along the inner conductor and a current $-I_o$ flows along the shield. These total currents distribute themselves, on the surface of the inner conductor and on the surface of the shield, in such a manner that the normal magnetic field vanishes at both surfaces. This current distribution will give rise to a magnetic field only in the space between the cable and the shield. Of course the field distribution we are talking about is independent of z and, in any plane perpendicular to z, it is just the transverse magnetic field distribution of the TEM mode of propagation within the cable-shield structure. Now let this auxiliary magnetic field distribution, $\underline{H}_o$, be equal to the gradient of a magnetic potential, Ω_o. Since there is a current I_o flowing on the inner conductor, we will have to define an infinite surface joining the inner conductor to the shield across which Ω_o jumps by a value I_o. Let this jump surface be the same one through which we desire to calculate the difference

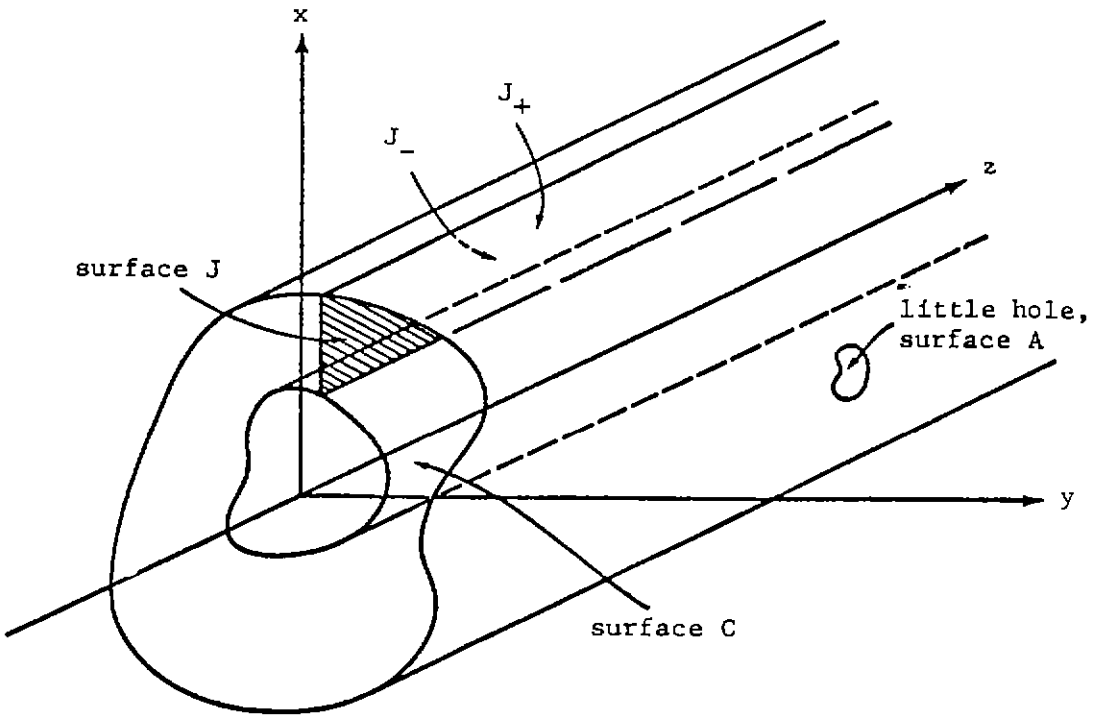

Figure 1. Infinitely long shielded cable with a little hole.

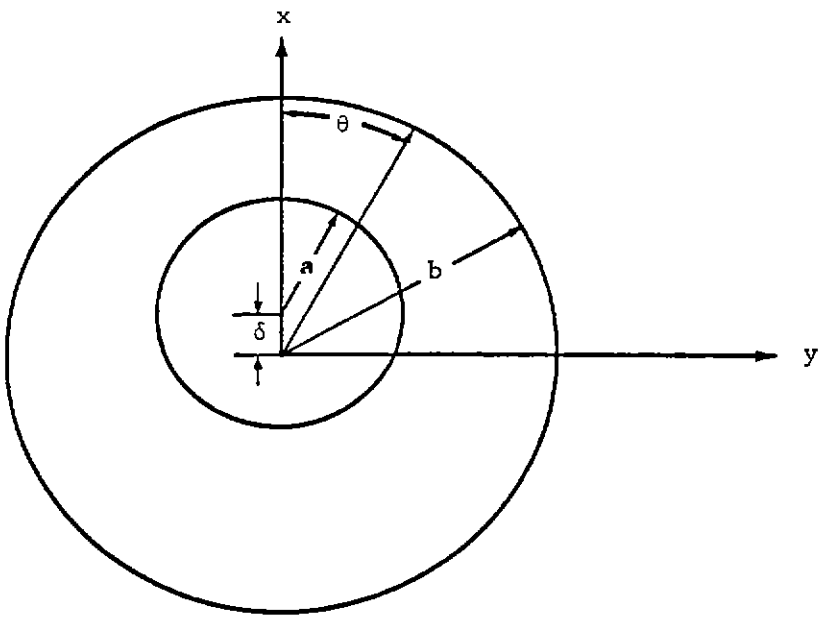

Figure 2. Cross-section of a particular example of figure 1.

flux in the main problem.

Now let us return to the main problem where a net current I_s flows in the shield with a hole and a net current I flows on the inner conductor. Here one can say that the difference magnetic field in the space between the cable and the shield, $\underline{H}$, can be derived from another magnetic potential, Ω, and that there is no jump surface joining the inner conductor to the shield; Ω is continuous throughout the region.

Both Ω and Ω_o satisfy Laplace's equation, therefore ([5], p. 54, eq. 4)

$$\int \Omega \frac{\partial \Omega_o}{\partial n} \, dS = \int \Omega_o \frac{\partial \Omega}{\partial n} \, dS \tag{2.1}$$

where $\underline{n}$ is the outward normal from the field region and the integrals are over the inner surface of the shield, the outer surface of the inner conductor, and both sides of the jump surface. The integrand of the left hand side of equation (2.1) vanishes over all surfaces, and the integrand of the right hand side vanishes over all surfaces except A, the aperture region of the shield, and J, the jump surface. Thus,

$$\int_{J_+} \Omega_o \frac{\partial \Omega}{\partial n} \, dS + \int_{J_-} \Omega_o \frac{\partial \Omega}{\partial n} \, dS = - \int_A \Omega_o \frac{\partial \Omega}{\partial n} \, dS$$

Now, because of the difference in the direction of the normals,

$$\left(\frac{\partial \Omega}{\partial n}\right)_{J_-} = - \left(\frac{\partial \Omega}{\partial n}\right)_{J_+} ,$$

and so we have

$$\int_{J_+} (\Omega_o^+ - \Omega_o^-) \frac{\partial \Omega}{\partial n} \, dS = - \int_A \Omega_o \frac{\partial \Omega}{\partial n} \, dS.$$

But the clockwise difference flux through J is just

$$\Phi = - \mu_o \int_{J_+} \frac{\partial \Omega}{\partial n} \, dS,$$

while

$$\Omega_o^+ - \Omega_o^- = -I_o,$$

Thus, an alternative expression for the total difference flux is

$$\Phi = -\frac{\mu_o}{I_o}\int_A \Omega_o \frac{\partial \Omega}{\partial n}\, dS,$$

and the equivalent voltage source of the hole, V_{eq}, is just

$$V_{eq} = i\omega\Phi = -i\omega\mu_o \int_A \left(\frac{\Omega_o}{I_o}\right) H_n dS \tag{2.2}$$

where H_n is the outward normal component of the magnetic field in the hole and a harmonic time dependence of the form $\exp(-i\omega t)$ has been assumed and suppressed. Equation (2.2) is rigorous, under the low frequency assumption, for any size of aperture. We will now make the assumption that the hole is small and expand Ω_o in a Taylor series in s, the counterclockwise arc length along a shield cross-section, about some point, s_h, chosen as the center of the hole. Keeping only two terms in the expansion, we have

$$V_{eq} = -i\omega\mu_o \int_A \left\{ \frac{\Omega_o(s_h)}{I_o} + \left.\frac{\partial \Omega_o}{\partial s}\right|_{s_h} \cdot \frac{(s-s_h)}{I_o} \right\} H_n(s,z)dS. \tag{2.3}$$

But, applying equation (2.1), with Ω_o replaced by a constant, it is clear that

$$\int_A H_n(s,z)dS = 0,$$

while

$$\left.\frac{\partial \Omega_o}{\partial s}\right|_{s_h} = -K_o(s_h),$$

where $K_o(s_h)$ is the surface current density at s_h in the auxiliary problem. Thus equation (2.3) may be written as

$$V_{eq} = i\omega\mu_o \frac{K_o(s_h)}{I_o} \int_A s H_n(s,z)dS \tag{2.4}$$

Let us define a dimensionless, positive, density function, $d_i(s)$, through

$$K_o(s) = -\frac{I_o}{P} d_i(s)$$

where P is the perimeter of the cross-section of the shield. The density function, $d_i(s)$, is the ratio of the surface current of the auxiliary problem at point s to the average surface current of the auxiliary problem. Using this definition, one can write equation (2.4) as

$$V_{eq} = -\frac{i\omega\mu_o d_i(s_h)}{P} \int_s sH_n(s,z)dS \qquad (2.5)$$

The effective magnetic dipole moment of the hole is defined by the integral remaining in equation (2.5). This corresponds to the usual definition of the effective induced dipole moment in a hole in an infinite conducting plane, as may be seen by using an appropriate half-space Green's function to write the magnetic potential of the field penetrating the hole in the plane as

$$\Omega(\underline{r}) = \frac{1}{2\pi} \int \frac{H_n(\underline{r}')}{|\underline{r}-\underline{r}'|} dS',$$

where the integral is over the hole. Far from the hole in the plane, one may write

$$\Omega(\underline{r}) = \frac{1}{2\pi r} \int H_n(\underline{r}')dS' + \frac{1}{2\pi} \frac{\underline{r}}{r^3} \cdot \int \underline{r}' H_n(\underline{r}')dS'$$

$$= \frac{\underline{r}\cdot\underline{m}_{eff}}{2\pi r^3},$$

where

$$\underline{m}_{eff} = \int \underline{r}' H_n(\underline{r}')dS'.$$

Thus, by analogy, the integral in equation (2.5) is the transverse component of the effective magnetic dipole induced in the hole. Since we will only be concerned with this transverse component of the effective magnetic dipole, and the holes we will be concerned with have a plane of symmetry perpendicular to the cable axis, we will treat the dipole as a scalar quantity and write

$$\int_A sH_n(s,z)dS = m_{eff}.$$

If the hole is small, the value of m_{eff} will be made up of two main parts. One part is proportional to the external surface current at the position of the center of the hole when the hole is closed and the other part is proportional to the internal surface current at the position of the center of the hole when the hole is closed. Of course, one could speak of tangential magnetic fields in place of surface currents. Now if $K_{ext}(s)$ is the exterior surface current, one can define an exterior density function, $d_e(s)$, through

$$K_{ext}(s) = \frac{I_T}{P} d_e(s)$$

where I_T is the total current flowing on the shielded cable. Based on our basic assumption that all wavelengths of interest are much longer than a cable dimeter, it is not difficult to see that $d_e(s)$ is independent of the excitation of the exterior current; a given current, I_T, will distribute itself over the surface in the same manner for any excitation field of low frequency. The interior surface current with the hole closed is just

$$K_{int}(s) = -\frac{I}{P} d_i(s)$$

Now, adding the two contributions to m_{eff}, one obtains

$$m_{eff} = P^{-1}[\alpha_m^{ext} I_T d_e(s_h) - \alpha_m^{int} I d_i(s_h)]$$

where the proportionality constants, α_m^{ext} and α_m^{int}, are the exterior and interior "polarizabilities" of the hole. One can use an equation like (2.1) to show that as long as the hole is small enough for equation (2.5) to be valid, then

$$\alpha_m^{ext} = \alpha_m^{int} \equiv \alpha_m,$$

and so

$$m_{eff} = \alpha_m P^{-1}[I_T d_e(s_h) - I d_i(s_h)] \qquad (2.6)$$

Previous work in this area has approximated α_m by defining an elliptical hole "equivalent" to the real hole and placing the elliptical hole in an infinite plane. In Sections VI through IX of this note, we will discuss four factors that it is necessary to consider if a more accurate estimate of the hole polarizability is to be made.

Now, using equation (2.6), equation (2.5) may be rewritten as

$$V_{eq} = - \frac{i\omega\mu_o\alpha_m u_i(s_h)}{p^2} [d_e(s_h)I_T - d_i(s_h)I]. \tag{2.7}$$

If one has in mind an analysis of fairly good shields, then I will be much smaller than I_T and the density functions will be approximately equal, so one can quite accurately write

$$V_{eq} = - i\omega\mu_o\alpha_m \frac{d_i(s_h)d_e(s_h)}{p^2} I_s \tag{2.8}$$

This is our final form for the equivalent voltage source of a single small hole in a cable shield. We now turn to some simple specific examples of the application of equation (2.8).

The simplest possible application is to a cable and shield making up a circular cylindrical coaxial system. If the radius of the shield cylinder is b, equation (2.8) reduces to

$$V_{eq} = - \frac{i\omega\mu_o\alpha_m I_s}{(2\pi b)^2} \tag{2.9}$$

since, for the structure in question, $d_i(s) = d_e(s) = 1$.

A slightly more complicated example occurs if the cable and shield are again circular cylinders, but the axis of the inner conductor is shifted a distance δ from the axis of the shield. Such a situation is shown in cross-section in figure 2, where a is the radius of the inner conductor and b is the radius of the shield. In such a case $d_e(s)$ is still unity but $d_i(s)$ is no longer unity. If the θ of figure 2 is used as the parameter of arc length, it can be shown by conformal transformation techniques (e.g. by a slight reshuffling of the results in [5], §4.13) that

$$d_i(\theta) = \frac{\sqrt{1-\beta^2}}{1-\beta \cos \theta} \tag{2.10}$$

where

$$\beta = \frac{2\delta b}{b^2-a^2+\delta^2} .$$

Thus, in this case,

$$V_{eq} = - \frac{i\omega\mu_o\alpha_m d_i(\theta_h)}{(2\pi b)^2} \cdot I_s$$

where θ_h is determined by the position of the center of the hole.

This concludes our preliminary discussion of the equivalent voltage sources of little holes. Now we turn to a derivation of their equivalent current sources.

III. Current Source of One Little Hole in a Cable Shield

The geometrical configuration of the problem to be studied is the same as in the previous section. Figure 1 is again the relevant diagram.

The strength of the equivalent current source of the hole is given by $i\omega$ multiplied by the difference charge on the inner conductor when a static linear charge density Q_s exists on the shield far from the hole and a static linear charge density Q exists on the inner conductor far from the hole. Again this follows from appropriate limits of previous results [3]. By "difference charge" in the above definition, we mean the total charge minus the charge that would exist on the inner cable if the hole were closed. The boundary-value problem implied by the above definition will be called the main problem of this section.

As in the previous section, we can arrive at an alternative way of calculating the strength of the equivalent current source by considering an auxiliary boundary-value problem — the one where the hole is closed and a linear charge density Q_o exists on the cable and a linear charge density $-Q_o$ exists on the shield. These linear charge densities distribute themselves, over their respective surfaces, in such a manner that the tangential electric field vanishes at both surfaces. The field between the cable and the shield is just the transverse electric field distribution of the TEM mode of propagation within the cable-shield structure. This electric field distribution may be set equal to the negative gradient of an electrostatic potential, ϕ_o. Without any loss of generality we can set ϕ_o equal to zero on the surface of the shield and equal to Q_o/C_o on the surface of the cable, where C_o is the capacitance per unit length of the TEM structure of the auxiliary problem. The auxiliary boundary-value problems of the previous section and of this section are, of course, quite closely related. They are both really two-dimensional problems, and their potentials are the real and imaginary parts of a single analytic function. Thus the two problems can actually be solved simultaneously.

Now let us return to the main problem and set the difference electric field equal to the negative gradient of another electrostatic potential, ϕ, in the whole region between the cable and the shield. Without any loss of generality we can set ϕ equal to zero on both the metallic portion of the shield surface and the entire surface of the inner conductor. For simplicity of presentation , in this note we will assume that the permittivity is equal to that of free space

throughout the entire region of interest.

Both ϕ and ϕ_o satisfy Laplace's equation, therefore ([5], p. 54, eq. 4)

$$\int \phi_o \frac{\partial \phi}{\partial n} \, dS = \int \phi \frac{\partial \phi_o}{\partial n} \, dS, \tag{3.1}$$

where $\underline{n}$ is the outward normal from the field region and the integrals are over the shield surface and the surface of the inner conductor.

The integrand of the left-hand side of equation (3.1) vanishes over the shield while the integrand of the right-hand side vanishes everywhere except over the aperture in the shield. Therefore,

$$\int_C \phi_o \frac{\partial \phi}{\partial n} \, dS = \int_A \phi \frac{\partial \phi_o}{\partial n} \, dS.$$

But the difference charge on the inner cable in the main problem is just

$$\varepsilon_o \int_C \frac{\partial \phi}{\partial n} \, dS.$$

Thus an alternative expression for the difference charge is

$$Q_D = \frac{\varepsilon_o C_o}{Q_o} \int_A \phi \frac{\partial \phi_o}{\partial n} \, dS,$$

and the equivalent current source of the hole, I_{eq}, is just

$$I_{eq} = i\omega Q_D = i\omega \varepsilon_o C_o \int_A \frac{1}{Q_o} \frac{\partial \phi_o}{\partial n} \, dS \tag{3.2}$$

By considering the auxiliary electrostatic problem a little more closely it becomes clear that, on the inner surface of the shield,

$$\frac{1}{Q_o} \frac{\partial \phi_o}{\partial n} = - \frac{d_i(s)}{P\varepsilon_o} \tag{3.3}$$

where $d_i(s)$ is the same inner density function introduced in the previous section. This function can be computed by solving either the electrostatic or the magnetostatic auxiliary problems since, as is well known, the surface charge density of the electrostatic problem is proportional to the surface current density of

the magnetostatic problem.

By substituting equation (3.3) into equation (3.2), one obtains

$$I_{eq} = - \frac{i\omega C_o}{P} \int_A \phi(s,z) d_i(s) dS \tag{3.4}$$

This equation is valid for any size of hole. By specializing to small holes it is possible to bring the density function outside the integral and thus to write

$$I_{eq} = - \frac{i\omega d_i(s_h) C_o}{P} \int_A \phi(s,z) dS \tag{3.5}$$

For reasons similar to those given in the previous section in the discussion of the effective magnetic dipole of the hole, the remaining integral in equation (3.5) is proportional to the effective electric dipole of the aperture. More precisely, we have

$$p_{eff} = \alpha_e P^{-1} [Q_T d_e(s_h) - Q d_i(s_h)], \tag{3.6}$$

where α_e is the electric polarizability of the hole. Four of the factors that determine the magnitude of α_e will be discussed in Sections VI through IX.

By making use of equation (3.6), equation (3.5) may now be rewritten as

$$I_{eq} = i\omega(C_o/\varepsilon_o) \frac{\alpha_e d_i(s_h)}{P^2} [Q_T d_e(s_h) - Q d_i(s_h)] \tag{3.7}$$

and, as in the previous section, for the purposes of studying shielding by small holes it is quite accurate to write

$$I_{eq} = i\omega(C_o/\varepsilon_o) \frac{\alpha_e d_i(s_h) d_e(s_h)}{P^2} Q_s. \tag{3.8}$$

This is our final form for the equivalent current source of a single small hole in a cable shield.

The simplest application of equation (3.8) is to a cable and shield that are coaxial circular cylinders. In that case, if a is the radius of the cable and b is the radius of the shield, we have

$$C_o = \frac{2\pi\varepsilon_o}{\ln(b/a)} ,$$

and thus it follows easily that

$$I_{eq} = \frac{i\omega\alpha_e Q_s}{2\pi b^2 \ln(b/a)} \tag{3.9}$$

For the "off-center coax" whose cross-section is shown in figure 2, we have ([5], §4.13)

$$C_o = \frac{2\pi\varepsilon_o}{\cosh^{-1}(\gamma)}$$

where

$$\gamma = \frac{b^2+a^2-\delta^2}{2ab} .$$

Thus, for a small hole in this off-center cylindrical shield,

$$I_{eq} = \frac{i\omega\alpha_e d_i(\theta_h) Q_s}{2\pi b^2 \cosh^{-1}(\gamma)} \tag{3.10}$$

where $d_i(\theta_h)$ is given by equation (2.10).

IV. The Two Sources Combined

In order to see how the results of Sections II and III can be used to solve shielding problems, and also to understand a little about the combined effect of the two types of source, let us look at the relatively simple problem of an infinitely long cable within an infinitely long, circular cylindrical shield, of radius b, containing a single small hole. We will suppose that this cable and shield are immersed in an external, time-harmonic, plane wave whose propagation vector makes an angle θ_i with the axis of the shielded cable (the z-axis) and whose magnetic field is perpendicular to the axis of the cable. This situation is shown schematically in figure 3. It is assumed that the wavelength of the incident wave is much larger than a cable diameter.

The procedure to be used is to solve the external scattering problem with the hole closed, and then to determine, from this solution, the total current and the linear charge density at the position of the hole. This current and charge will determine the equivalent voltage and current sources of the hole through equations (2.8) and (3.8) because, with the hole closed, the total current and charge will be equal to the shield current and charge. These equivalent voltage and current sources are to be used in conjunction with the equivalent transmission-line circuit shown in figure 4. The transmission-line current of the equivalent circuit is the total current on the inner cable. The transmission-line voltage of the equivalent circuit is the voltage between the cable and its shield. The justification of this procedure can be based on arguments quite similar to those presented in reference 3.

If the incident magnetic field is given by

$$\underline{H}^{inc} = -\underline{e}_y H e^{ik(z \cos \theta_i + x \sin \theta_i)},$$

the solution of the scattering problem ([6], chaps. 1 and 2) leads to a total current given by

$$I_T(z) = I_s(z) = e^{ikz \cos \theta_i} \frac{4H}{k \sin \theta_i H_o^{(1)}(kb \sin \theta_i)} . \qquad (4.1)$$

We also have available the relation, valid for plane-wave scattering from

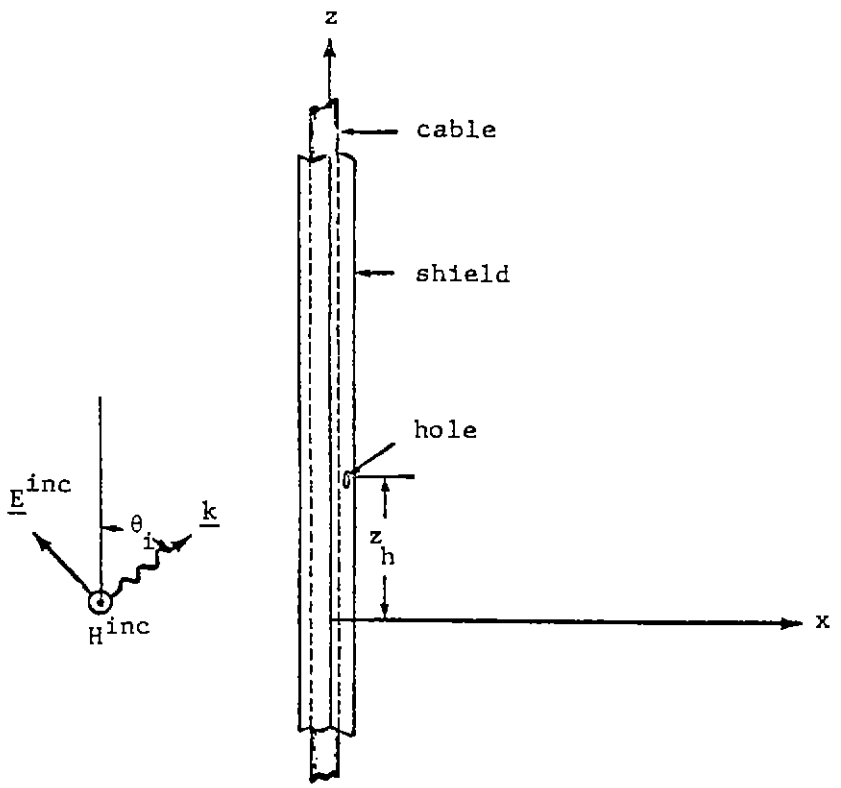

Figure 3. A plane wave incident on an infinitely long shielded cable with a small hole.

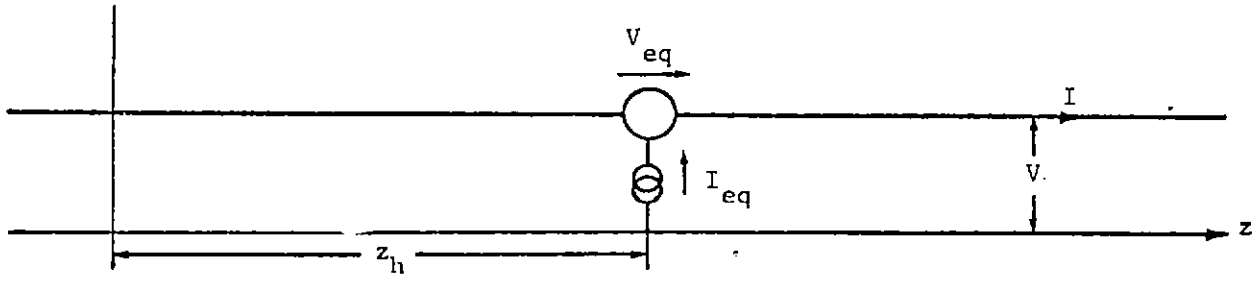

Figure 4. Transmission-line equivalent circuit for shielded cable with a small hole.

infinitely long shielded cables,

$$Q_s(z) = Q_T(z) = \frac{\cos\theta_i I_T(z)}{c} . \tag{4.2}$$

Relation (4.2) between the total current and the linear charge density is true for any shape of shield cross-section since, for the scattering problem under consideration, all quantities vary with z according to $\exp(ikz\cos\theta_i)$, and a substitution of this type of variation into the rigorous equation

$$\frac{dI_t}{dz} = i\omega Q_T$$

leads directly to equation (4.2).

We have called our shield an infinite circular cylinder, and given the explicit equation for $I_T(z)$, (4.1), merely as an example of a calculation of $I_T(z)$. In the rest of this section it will only be necessary to invoke the general relation for infinite cables, (4.2). Of course, for shielded cables of finite length the z-dependence of I_T would be more complex than that given by equation (4.1), and equation (4.2) would no longer hold.

Now let us turn to the calculation of the transmission-line currents and voltages generated by the two sources of figure 4. With these two sources present the transmission-line equations take the form

$$\frac{dV}{dz} = i\omega L_o I + V_{eq}\delta(z)$$

$$\frac{dI}{dz} = i\omega C_o V + I_{eq}\delta(z)$$

where L_o and C_o are the inductance and capacitance per unit length as computed from the auxiliary problems of sections II and III. The separated, second-order equations for voltage and current are

$$\frac{d^2V}{dz^2} + k^2V = i\omega L_o I_{eq}\delta(z - z_h) + V_{eq}\delta'(z - z_h) \tag{4.3}$$

$$\frac{d^2I}{dz^2} + k^2I = i\omega C_o V_{eq}\delta(z - z_h) + I_{eq}\delta'(z - z_h) \tag{4.4}$$

where the relation

$$\omega^2 L_o C_o = k^2$$

has been used.

The first source term of equation (4.3) gives rise to a voltage wave given by ([7], chap. 7)

$$V_1 = i\omega L_o I_{eq} \frac{e^{ik|z-z_h|}}{2ik}, \tag{4.5}$$

while the second source term in equation (4.3) gives rise to a second voltage wave given by (this can be obtained by differentiation of the voltage wave for a delta-function source)

$$V_2 = V_{eq}[U(z - z_h) - \tfrac{1}{2}]e^{ik|z-z_h|}, \tag{4.6}$$

where $U(z)$ is the unit step function of z. Thus, by superposition, the total transmission-line voltage is

$$V = \left\{cL_o I_{eq} + V_{eq}[2U(z - z_h) - 1]\right\} \frac{e^{ik|z-z_h|}}{2} \tag{4.7}$$

Similarly, one can show that

$$I = \left\{cC_o V_{eq} + I_{eq}[2U(z - z_h) - 1]\right\} \frac{e^{ik|z-z_h|}}{2} \tag{4.8}$$

Substituting equations (2.8) and (3.8) into equations (4.7) and (4.8) we have

$$V = i\omega \frac{d_i(s_h)d_e(s_h)}{p^2} \left\{\frac{\alpha_e cL_o C_o Q_s(z_h)}{\epsilon_o} - \alpha_m \mu_o I_s(z_h)[2U(z - z_h) - 1]\right\} \frac{e^{ik|z-z_h|}}{2}$$

$$I = i\omega \frac{d_i(s_h)d_e(s_h)}{p^2} \left\{-\alpha_m cC_o \mu_o I_s(z_h) + \frac{\alpha_e C_o Q_s(z_h)}{\epsilon_o}[2U(z - z_h) - 1]\right\} \frac{e^{ik|z-z_h|}}{2}.$$

By invoking equation (4.2), and by defining

$$V_o = \frac{-i\omega d_i(s_h)d_e(s_h)I_T(z_h)}{p^2},$$

the equations for V and I simplify to

$$V = -V_o\left\{\alpha_e \cos\theta_i - \alpha_m[2U(z - z_h) - 1]\right\}\frac{e^{ik|z-z_h|}}{2} \tag{4.9}$$

$$I = -V_o Y_o\left\{-\alpha_m + \alpha_e \cos\theta_i[2U(z - z_h) - 1]\right\}\frac{e^{ik|z-z_h|}}{2}, \tag{4.10}$$

where

$$Y_o \equiv \sqrt{C_o/L_o}$$

An interesting special case arises if the hole is a long, narrow slit whose length is still much less than a wavelength and whose longer dimension is parallel to the z-axis. For such a slit it can be shown [2] that α_m and α_e are equal, and so we have

$$V = \frac{1}{2} V_o\alpha_e[2U(z - z_h) - (1 + \cos\theta_i)]e^{ik|z-z_h|} \tag{4.11}$$

$$I = \frac{1}{2} V_o Y_o\alpha_e[2\cos\theta_i U(z - z_h) - (1 + \cos\theta_i)]e^{ik|z-z_h|} \tag{4.12}$$

From these equations one can see that at broad-side incidence ($\theta_i = \pi/2$) half the energy penetrating the hole travels in the positive z-direction inside the shield and the other half travels in the negative z-direction. As the angle of incidence becomes larger, more and more of the penetrating energy travels in the positive z direction until finally, as θ_i approaches π, all of the penetrating energy goes in the positive z direction. A study of equations (4.9) and (4.10) reveals that a similar kind of thing happens for an arbitrarily shaped hole, but the penetrating energy never quite goes completely in one direction since α_m is greater than α_e except for narrow axial slits.

In the general case the ratio of the amount of energy traveling in the more favored direction to the amount traveling in the less favored direction is given by the expression,

$$\left|\frac{\alpha_m+\alpha_e|\cos\theta_i|}{\alpha_m-\alpha_e|\cos\theta_i|}\right|^2.$$

In this section we have seen how the direction of propagation of the greater portion of the energy within the shield depends on the combined effect of the two equivalent-sources of the hole.

V. A Braided Shield Model

In Sections II and III we found expressions for the equivalent voltage and current sources for a single small hole in terms of the polarizabilities of the hole. We took the basic definitions of the voltage and current sources in terms of flux and charge from some previous work on periodic shields [3]. In this section we wish to return the spatial periodicity to the shielded cable and thus eventually to arrive at a model for a braided shield. The results we will arrive at here could also have been obtained directly, but it was decided that the results for a single hole might be of more general interest than the results for an array of holes, and so the single-hole results have been presented *first*.

As a preliminary we note that, from previous work on periodic shields ([3], eq. 7)

$$\frac{dV}{dz} = i\omega LI + i\omega L_s I_T \tag{5.1}$$

where, by definition, $L\Delta$ is the flux in one period of length Δ that lies within the shield and circulates the cable when one ampere flows on the cable and returns through the shield. Also by definition, $L_s\Delta$ is the flux in one period of length Δ that lies within the shield and circulates the cable when one ampere flows on the shield and no net current flows on the cable inside.

Now let us consider an infinite row of identical small holes in the shield as shown in figure 5. The holes are a distance Δ apart. Suppose a current I flows on the cable and a current I_s flows on the shield, and let I_T be their sum. Let us write the difference field (defined in Section II) due to the m^{th} hole, when these currents flow, as

$$\underline{H}_D(x,y,z - m\Delta).$$

Now let us calculate $\Phi(\Delta)$, the clockwise flux that lies within the shield and circulates the cable in one period of length Δ. This flux is the integral of a field that is made up of $\underline{H}_o(x,y,z)$, the field of the auxiliary problem of Section II (i.e. the field with all the holes closed and a current I_o on the

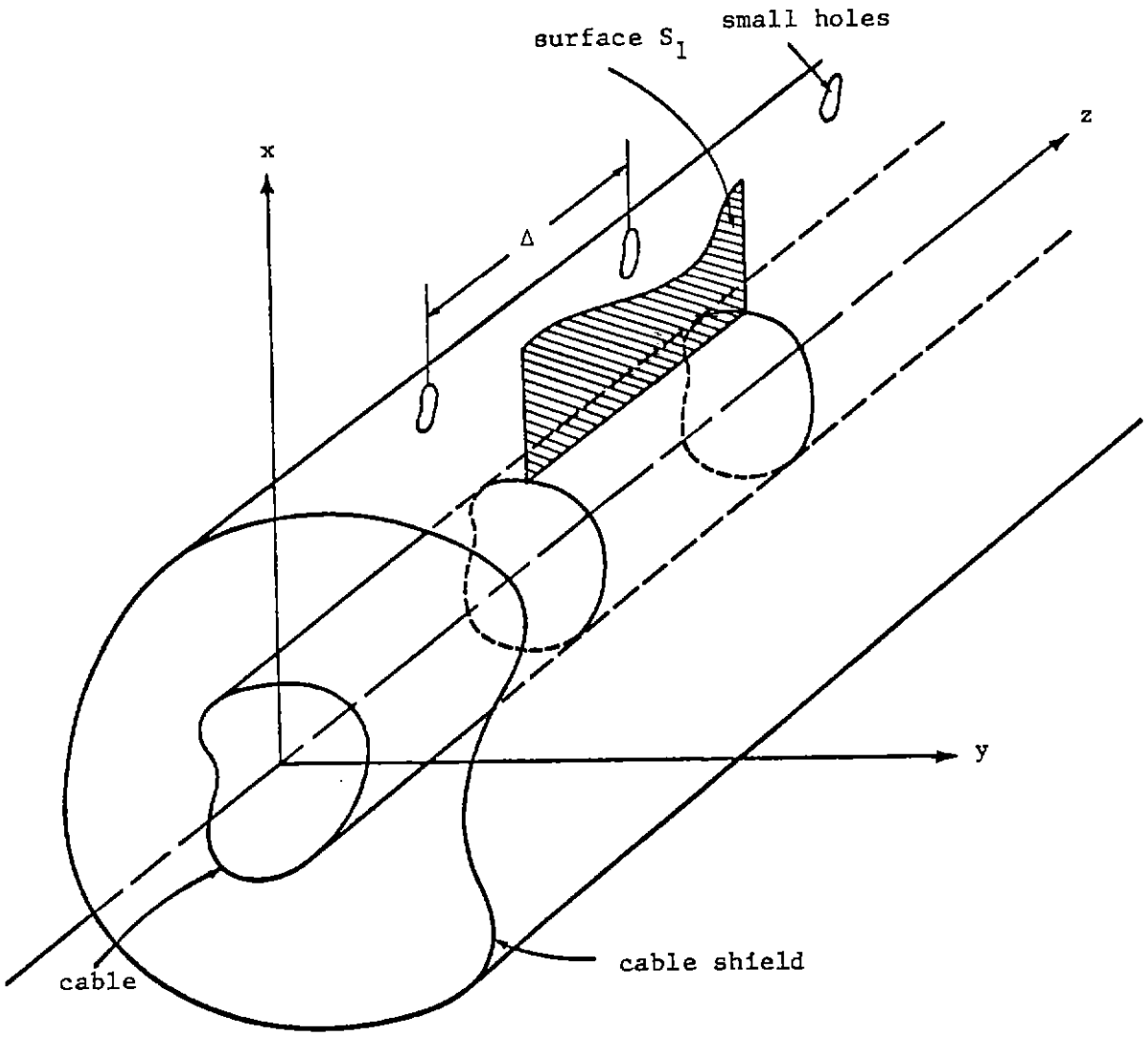

Figure 5. A shield with a row of small holes.

inner cable), and the sum of the difference fields of all the holes. Thus

$$\Phi(\Delta) = \mu_o \frac{I}{I_o} \int_{S_1} \underline{H}_o \cdot d\underline{S} + \mu_o \int_{S_1} \sum_{m=-\infty}^{\infty} \underline{H}_D(x,y,z - m\Delta) \cdot d\underline{S}$$

where S_1 is a surface such as that shown in figure 5. But, by recalling the definition of L_o from Section IV, and by interchanging the summation and integration,

$$\Phi(\Delta) = L_o \Delta I + \mu_o \sum_{m=-\infty}^{\infty} \int_{S_1} \underline{H}_D(x,y,z - m\Delta) \cdot d\underline{S}$$

$$= L_o \Delta I + \mu_o \int_{S_\infty} \underline{H}_D(x,y,z) \cdot d\underline{S} \qquad (5.2)$$

where S_∞ is the infinite surface made up of the surfaces in each period that are equivalent to S_1. We have already considered the integral of equation (5.2) in Section II and hence, from equation (2.7) divided by $i\omega$, we can write the following equivalent expression for $\Phi(\Delta)$:

$$\Phi(\Delta) = \left\{ L_o + \frac{\mu_o \alpha_m d_i^2(s_h)}{P^2 \Delta} \right\} \Delta I - \frac{\mu_o \alpha_m d_i(s_h) d_e(s_h)}{P^2} I_T \qquad (5.3)$$

Now suppose there are N rows of identical holes spaced around the periphery of the shield at points $s_1, s_2, \cdots, s_j, \cdots s_N$. By superposing the effects of the individual rows, it is easy to see that we now have

$$\Phi(\Delta) = \left\{ L_o + \frac{\mu_o \alpha_m}{\Delta P^2} \sum_{j=1}^{N} d_i^2(s_j) \right\} \Delta I - \frac{\mu_o \alpha_m}{P^2} \sum_{j=1}^{N} d_i(s_j) d_e(s_j) \; I_T \qquad (5.4)$$

Thus it follows from the definitions of the terms in equation (5.1) that L, the inductance per unit length, is given by

$$L = L_o + \frac{\mu_o \alpha_m}{\Delta P^2} \sum_{j=1}^{N} d_i^2(s_j), \qquad (5.5)$$

and that L_s, the inductive coupling coefficient per unit length, is given by

$$L_s = - \frac{\mu_o \alpha_m}{\Delta P^2} \sum_{j=1}^{N} d_i(s_j) d_e(s_j). \qquad (5.6)$$

The number of holes per unit length, ν, is given by

$$\nu = N/\Delta,$$

therefore, if we define some average density functions through

$$\langle d_i^2 \rangle = \frac{1}{N} \sum_{j=1}^{N} d_i^2(s_j)$$

$$\langle d_i d_e \rangle = \frac{1}{N} \sum_{j=1}^{N} d_i(s_j) d_e(s_j),$$

we can rewrite equations (5.5) and (5.6) as

$$L = L_o + \frac{\mu_o \nu \alpha_m}{p^2} \langle d_i^2 \rangle \tag{5.7}$$

$$L_s = - \frac{\mu_o \nu \alpha_m}{p^2} \langle d_i d_e \rangle \tag{5.8}$$

If the shield is a circular cylinder we know that $d_e(s_j)$ is equal to unity, and so, if N is large and the holes are uniformly spaced around the shield's periphery,

$$-L_s = \frac{\mu_o \nu \alpha_m}{p^2} \langle d_i \rangle$$

$$\approx \frac{\mu_o \nu \alpha_m}{p^2} \frac{1}{P} \int_o^P d_i(s_j) = \frac{\mu_o \nu \alpha_m}{(2\pi b)^2} \tag{5.9}$$

This equation is an agreement with other results. The sum in the equation for L doesn't reduce as nicely as that in the equation for L_s unless the cable is a circular cylinder coaxial with the shield cylinder.

We turn now to the other transmission-line equation from [3],

$$\frac{dI}{dz} = i\omega CV - i\omega C S_s Q_T \tag{5.10}$$

where, by definition, Δ/C is the voltage between the shield and the cable when there is a charge of one coulomb per cable period on the cable and minus one coulomb per cable period on the shield. Also by definition, $-CS_s$, the capacitive coupling coefficient per unit length, is equal to the proportion of the charge on the cable when the cable and shield are at the same potential and their combination carries a charge Q_T per unit length.

By arguments completely analogous to those presented above in the flux calculation, one can use the results of Section III to say that the charge on the cable per period is given by

$$Q\Delta = VC_o\Delta + \frac{C_o\alpha_e}{\varepsilon_o P^2}\left(Q_T\langle d_i d_e\rangle - Q\langle d_i^2\rangle\right)$$

i.e.

$$Q = \frac{VC_o}{1+(C_o\alpha_e/\Delta\varepsilon_o P^2)\langle d_i^2\rangle} + \frac{Q_T(C_o\alpha_e/\Delta\varepsilon_o P^2)\langle d_i d_e\rangle}{1+(C_o\alpha_e/\Delta\varepsilon_o P^2)\langle d_i^2\rangle} \tag{5.11}$$

Thus, from the definitions of C and CS_s,

$$C = \frac{C_o}{1+(C_o\alpha_e/\Delta\varepsilon_o P^2)\langle d_i^2\rangle} \tag{5.12}$$

and

$$S_s = -\frac{\alpha_e}{\Delta\varepsilon_o P^2}\langle d_i d_e\rangle \tag{5.13}$$

or, in terms of ν, the number of holes per unit length,

$$C^{-1} = C_o^{-1} + \frac{\nu\alpha_e}{\varepsilon_o P^2}\langle d_i^2\rangle \tag{5.14}$$

$$-S_s = \frac{\nu\alpha_e}{\varepsilon_o P^2}\langle d_i d_e\rangle. \tag{5.15}$$

For circular cylindrical shields and large N, equation (5.15) reduced to

$$-S_s = \frac{\nu\alpha_e}{\varepsilon_o (2\pi b)^2}$$

We note that from equations (5.7) and (5.14) it is easy to show that

$$LC = L_o C_o \left\{ \frac{Z_o + Z_c \nu \alpha_m \langle d_i^2 \rangle / P^2}{Z_o + Z_c \nu \alpha_e \langle d_i^2 \rangle / P^2} \right\}$$

where

$$Z_o = \sqrt{L_o / C_o}$$

$$Z_c = \sqrt{\mu_o / \varepsilon_o},$$

thus we see that for thin axial slots ($\alpha_m = \alpha_e$) the propagation constant within the shield is equal to the free-space or TEM propagation constant.

It is also interesting to calculate the characteristic impedance of the line. This reduces to

$$Z = \sqrt{L/C} = Z_o \left\{ 1 + \frac{\nu^2 \alpha_m \alpha_e \langle d_i^2 \rangle^2}{P^4} + \frac{Z_c}{Z_o} \frac{\nu \langle d_i^2 \rangle}{P^2} (\alpha_m + \alpha_e) \right\}^{\frac{1}{2}}$$

We note in passing that the two other quantities defined in reference 3, L_c and S_c, are given by

$$L_c = L + L_s$$

$$= L_o + \frac{\mu_o \nu \alpha_m}{P^2} (\langle d_i^2 \rangle - \langle d_i d_e \rangle)$$

and

$$S_c = C^{-1} + S_s$$

$$= C_o^{-1} + \frac{\nu \alpha_e}{\varepsilon_o P^2} (\langle d_i^2 \rangle - \langle d_i d_e \rangle)$$

and thus, clearly, for the case where the cable and shield are coaxial cylinders ($d_i(s_j) = d_e(s_j) = 1$), we have $L_c = L_o$ and $S_c = C_o^{-1}$. This result has been mentioned previously [3]. We have given the above equations for L_c and S_c just to tie more closely together the work here with the previous work. We will make no further use of them in this note.

Let us now write our transmission-line equations in terms of the parameters usually used to describe braided shields [1]. Our model of the braided shield is a shield with a regular array of diamond-shaped holes, as shown in figure 6. The diamonds have internal angle 2ψ at the ends of their diagonals parallel to the cable axis. The centers of the holes lie along lines parallel to the cable axis and also along lines that could be drawn on the shield surface with pitch ψ.

From a look at the real braided shield that we are modelling, it is apparent that the number of holes per cable period is equal to the number of belts of wire in the braid. We denote this number by N (note that N is the number of belts going in both directions). It is easy to see that the cable period is given by

$$\Delta = \frac{2P}{N \tan \psi} \tag{5.16}$$

and thus

$$\nu = \frac{N}{\Delta} = \frac{N^2 \tan \psi}{2P} \tag{5.17}$$

If the length of the diamonds along the cable axis is denoted by δ, the optical coverage, c, is given by

$$c = 1 - (\delta/\Delta)^2. \tag{5.18}$$

If the width of a belt of wire is denoted by w (this is equal to the number of wires in a belt times the wire diameter under our assumption that the field leakage occurs mainly at the intersections between the belts), we have the relation

$$w = (\Delta - \delta)\sin \psi$$

or, by making use of equation (5.16)

$$\frac{\cos \psi}{N} = \frac{w}{2P(1-\delta/\Delta)} . \tag{5.19}$$

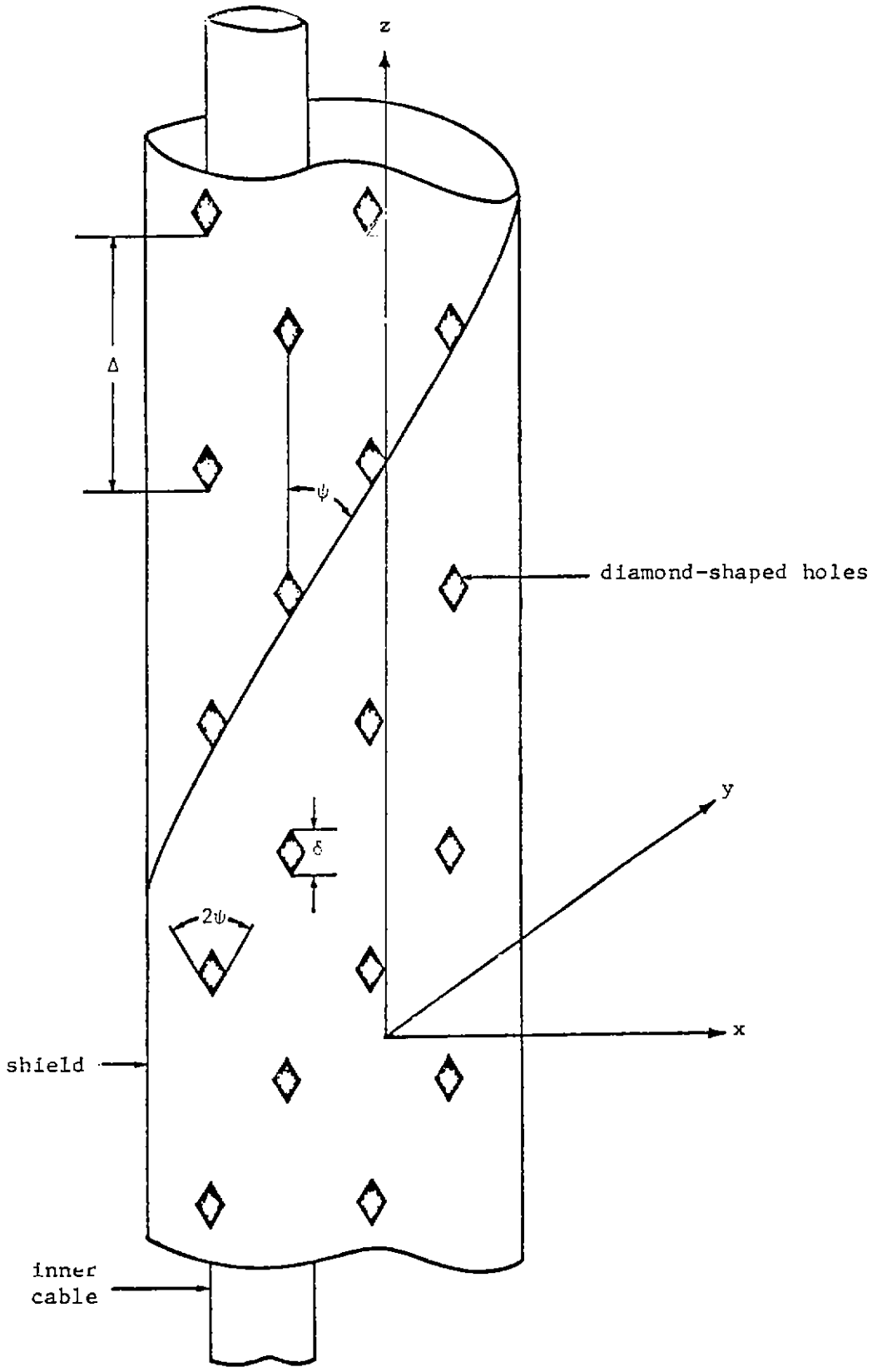

Figure 6. A model for a braided-shield cable.

We need one further definition. It will be seen in the next section that the electric polarizability of an isolated hole is almost proportional to A^2/P_h, where A is the area of the hole and P_h is the perimeter of the hole. We will normalize the electric polarizabilities of the holes with this factor and, in an attempt to be consistant, we will also normalize the magnetic polarizabilities with this factor. Although it will be found that the normalized magnetic polarizabilities depend quite strongly on the shape of the hole, the normalized electric polarizabilities are almost the same for any shape of hole. In any case, we now define $\bar{\alpha}_m(\psi)$ and $\bar{\alpha}_e(\psi)$, the normalized polarizabilities for the diamond-shaped holes we are particularly interested in, through

$$\alpha_m = \left(\frac{\delta}{2}\right)^3 \frac{\sin^2\psi}{\cos\psi}\,\bar{\alpha}_m(\psi) \tag{5.20}$$

$$\alpha_e = \left(\frac{\delta}{2}\right)^3 \frac{\sin^2\psi}{\cos\psi}\,\bar{\alpha}_e(\psi) \tag{5.21}$$

Now from equation (5.8) for L_s and the above set of parameters for a braid, it can easily be shown that

$$L_s = -\frac{\mu_o w}{P}\,\frac{(1-c)^{3/2}}{1-(1-c)^{1/2}}\,\bar{\alpha}_m(\psi)\langle d_i d_e\rangle. \tag{5.22}$$

If we approximate $\bar{\alpha}_m(\psi)$ by defining an equivalent ellipse, assume the shield is a circular cylinder, set the number of wires in a belt equal to one, and assume N is large, then equation (5.22) reduces to a previous result [1].

The equations for the other quantities of interest, L, S_s, and C, in terms of the braided shield parameters are also easily shown to be

$$L = L_o - L_s\,\frac{\langle d_i^2\rangle}{\langle d_i d_e\rangle} \tag{5.23}$$

$$S_s = -\frac{w}{\varepsilon_o P}\,\frac{(1-c)^{3/2}}{1-(1-c)^{1/2}}\,\bar{\alpha}_e(\psi)\langle d_i d_e\rangle \tag{5.24}$$

$$C^{-1} = C_o^{-1} - S_s\,\frac{\langle d_i^2\rangle}{\langle d_i d_e\rangle} \tag{5.25}$$

This completes our translation of the results of Sections II and III into the language of braided shields. Of all the equations in this section, the most relevant to braided shield calculations are equations (5.22) through (5.25) in conjunction with the transmission-line equations, (5.1) and (5.10). It will be seen that all we have really done is to reduce the problem to the calculation of $\overline{\alpha}_m(\psi)$ and $\overline{\alpha}_e(\psi)$. Although we have only indicated explicitly the variation of these quantities with ψ, they also depend on several other parameters. The study of some of these other factors will occupy us for the next four sections. We will see in the next section that if $\overline{\alpha}_m(\psi)$ had the value it would have for an isolated hole in a plane it would be a monotonically increasing function of ψ, but we will see in Section IX that if one takes into account the interactions among the holes, then $\overline{\alpha}_m(\psi)$ sometimes can have a minimum for some value of ψ other than zero. We will discuss more about this topic, and others, in Section X.

VI. Effect of Hole Shape on Hole Polarizabilities

In the second and third sections of this note, we have cast the problem of determining the effect of a small hole in a cable shield into the form of determining the hole polarizabilities, α_m and α_e. There are many factors that influence these quantities — the hole size and shape, the curvature of the surface in which it is located, etc. In this section we will discuss ways of determining what might be called the "basic" polarizabilities of holes. The basic polarizability of a hole will be defined as the polarizability of the hole when all factors except the hole size and shape are neglected, i.e. the polarizability of the hole when it is located in an infinite plane that is remote from all other conductors. The other factors influencing the hole polarizability will be treated as factors perturbing the basic polarizability. In some cases these "perturbations" will not be small, but the concept of basic polarizability is nevertheless useful as a tool for thinking about hole polarizability. In fact, that is the approximation to the exact polarizability that is usually used in discussing small hole effects. In the three sections following this one, we will discuss three types of perturbation of the basic polarizability. The perturbation discussed in Section IX can be quite strong in cases of practical interest.

The diamond-shaped holes of the braided shield model discussed in the previous section have a line of symmetry (actually they have two, but one is enough to make obvious the principal axes of the 2×2 polarizability tensor; this is really the simplification we want). The discussion of the present section will be restricted to holes with such symmetry for the sake of simplicity of notation in discussing α_m. The generalizations necessary for discussing unsymmetric holes will be apparent. We will assume a Cartesian coordinate system, locate the infinite plane in the x-y plane, and assume the line of symmetry of the hole to be along the x axis. This geometry is shown in figure 7, which is relevant to the determination of α_m for an arbitrary symmetric hole.

From Section II, and our definition of basic magnetic polarizability, one can see that that quantity can be determined by solving the magnetostatic boundary-value problem associated with figure 7:

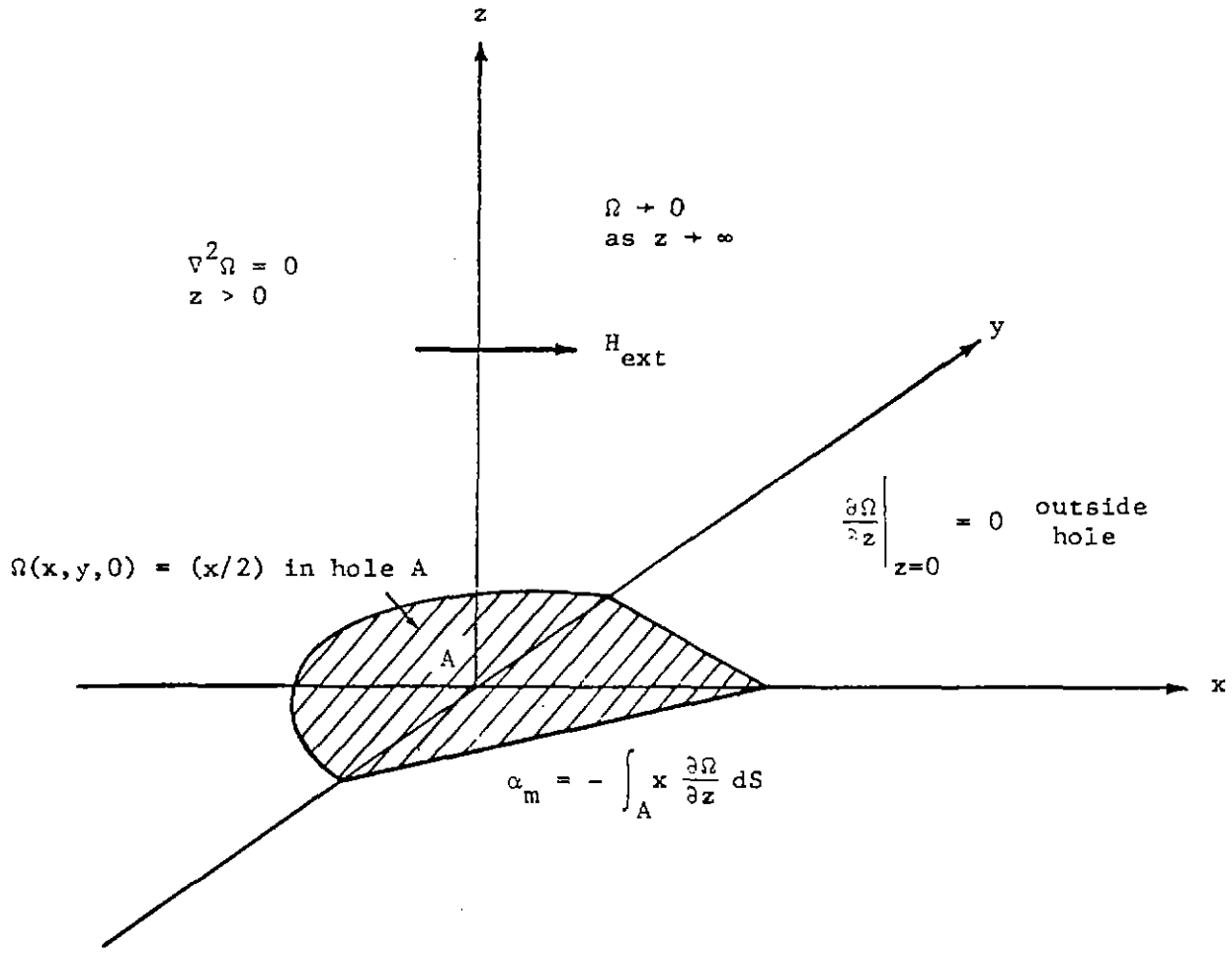

Figure 7. Boundary-value problem for determination of $\overline{\alpha}_m$.

$$\nabla^2 \Omega_T = 0$$

$$\Omega_T \to x, \qquad z \to \infty$$

$$\Omega_T \to 0, \qquad z \to -\infty$$

$$\frac{\partial \Omega_T}{\partial z} = 0, \qquad z = 0, \text{ outside the hole}$$

Ω_T and $(\partial \Omega_T)/(\partial z)$ are continuous through the hole, and then calculating the integral over the aperture, A,

$$\alpha_m = \int_A x \frac{\partial \Omega_T}{\partial z} \, dS \tag{6.1}$$

Now by writing

$$\Omega_T = x - \Omega(x,y,z) \qquad z > 0 \tag{6.2}$$

$$= \Omega(x,y,-z) \qquad z < 0 \tag{6.3}$$

one sees that all conditions on Ω_T are satisfied if

$$\nabla^2 \Omega = 0, \qquad z > 0$$

$$\Omega \to 0, \qquad z \to \infty$$

$$\frac{\partial \Omega}{\partial z}(x,y,0) = 0, \qquad \text{outside the hole}$$

$$\Omega(x,y,0) = (x/2), \qquad \text{in the hole}$$

Now, since Ω approaches zero sufficiently fast at infinity, it follows from Green's theorem that, for $z > 0$

$$\Omega(x,y,z) = \int \left\{ \Omega \frac{\partial G}{\partial z'} - G \frac{\partial \Omega}{\partial z'} \right\} dS' \tag{6.4}$$

where the integral is over the x-y plane, and G is an appropriate Green's function. Choosing $(\partial G/\partial z)$ to be zero on the x-y plane, we see that

$$\Omega(\underline{r}) = -\frac{1}{2\pi}\int_A \frac{1}{|\underline{r}-\underline{r}'|}\frac{\partial\Omega}{\partial z'}(x',y',0)dS' \tag{6.5}$$

Thus, allowing the field point to approach the hole and invoking the boundary condition on Ω in the hole, one arrives at the integral equation

$$x = \frac{1}{\pi}\int_A \frac{1}{\sqrt{(x-x')^2+(y-y')^2}}\left[-\frac{\partial\Omega}{\partial z'}(x',y',0)\right]dS'$$

Now, by defining

$$f(x,y) \equiv -\frac{\partial\Omega}{\partial z}(x,y,0) \tag{6.6}$$

and using the normalization of the previous section,

$$\bar{\alpha}_m = \frac{P_h}{A^2}\alpha_m, \tag{6.7}$$

our problem reduces to the determination of f by solving the integral equation

$$\frac{1}{\pi}\int_A\int \frac{f(x',y')}{\sqrt{(x-x')^2+(y-y')^2}}dx'dy' = x, \tag{6.8}$$

and the subsequent calculation of $\bar{\alpha}_m$ by performing the integral

$$\bar{\alpha}_m = \frac{P_h}{A^2}\int_A\int xf(x,y)dxdy \tag{6.9}$$

These calculations have been carried out numerically for both rectangular apertures and the diamond-shaped apertures that are of particular interest for our braided shield model. The calculations were carried out by dividing the aperture over which the integrations are to be performed into many small rectangular zones on which the unknown function, f, is assumed to be constant. The error in this procedure, once a definite perscription for the size and position of the rectangular zones as a function of N (the maximum number of zones

in a line parallel to the x-axis) is given, was assumed to be given implicitly, for large N, by the formula

$$\bar{\alpha}_m(N) = \alpha_m(\infty) + \frac{C_1}{N} + \frac{C_2}{N^2}$$

where C_1 and C_2 are constants. The value of $\bar{\alpha}_m(N)$ was calculated for three values of N, and the above formula was used to get a good approximation of the value of $\bar{\alpha}_m(\infty)$ $(=\bar{\alpha}_m)$. The results are presented in table I and figure 8.

The polarizability per unit length of a long uniform slot perpendicular to the magnetic field is well known to be given by the formula

$$\frac{\alpha_m}{\ell} = \frac{\pi}{16} w^2$$

where w is the width of the slot. From this fact it seems reasonable to assume that the normalized polarizability of a narrow slot whose width varies slowly along its length is given by

$$\bar{\alpha}_m \approx \frac{(\pi/8)\ell \int_0 w^2(y)dy}{\left[\int_0^\ell w(y)dy\right]^2} \qquad (6.10)$$

This formula was used to obtain the limiting forms of $\bar{\alpha}_m$ for thin rectangles and diamonds perpendicular to the magnetic field (given by $\pi/8$ and $\pi/6$ respectively) that are included in table I. For rectangles, an approximate empirical formula for the case where the longer side of the rectangle is perpendicular to the magnetic field is

$$\bar{\alpha}_m \approx \frac{\pi}{8}(1 + .55r) \qquad (6.11)$$

where r is the width to length ratio of the rectangle. Equation (6.11) is accurate to 3% for r less than 1/2.

We now turn to the calculation of α_e for an arbitrarily shaped hole in a plane. From Section III and our definition of basic electric polarizability, one can see that that quantity can be determined by solving the electrostatic boundary-value problem associated with figure 9,

Table 1a

$\bar{\alpha}_m$ for rectangles

width to-length ratio	$\bar{\alpha}_m$ (long side $\parallel$ to field)	$\bar{\alpha}_m$ (long side $\perp$ to field)
.00	∞	$\pi/8 = .393$
.05	41.274	
.10	14.239	.447
.15	7.984	
.20	5.430	.504
.25	4.091	
.30	3.283	.564
.35	2.752	
.40	2.377	.626
.45	2.096	
.50	1.883	.689
.55	1.717	
.60	1.588	.755
.65	1.473	
.70	1.378	.824
.75	1.297	
.80	1.232	.893
.85	1.174	
.90	1.124	.965
.95	1.078	
1.00	1.041	1.041

Table 1b

$\overline{\alpha}_m$ for diamonds

ψ, ½ angle of vertices on x-axis (degrees)	$\overline{\alpha}_m$
0	∞
5	35.256
10	10.773
15	5.509
20	3.467
25	2.444
30	1.854
35	1.478
40	1.225
45	1.041
50	.907
55	.805
60	.725
65	.665
70	.619
75	.582
80	.552
85	.533
90	$\pi/6$ = .524

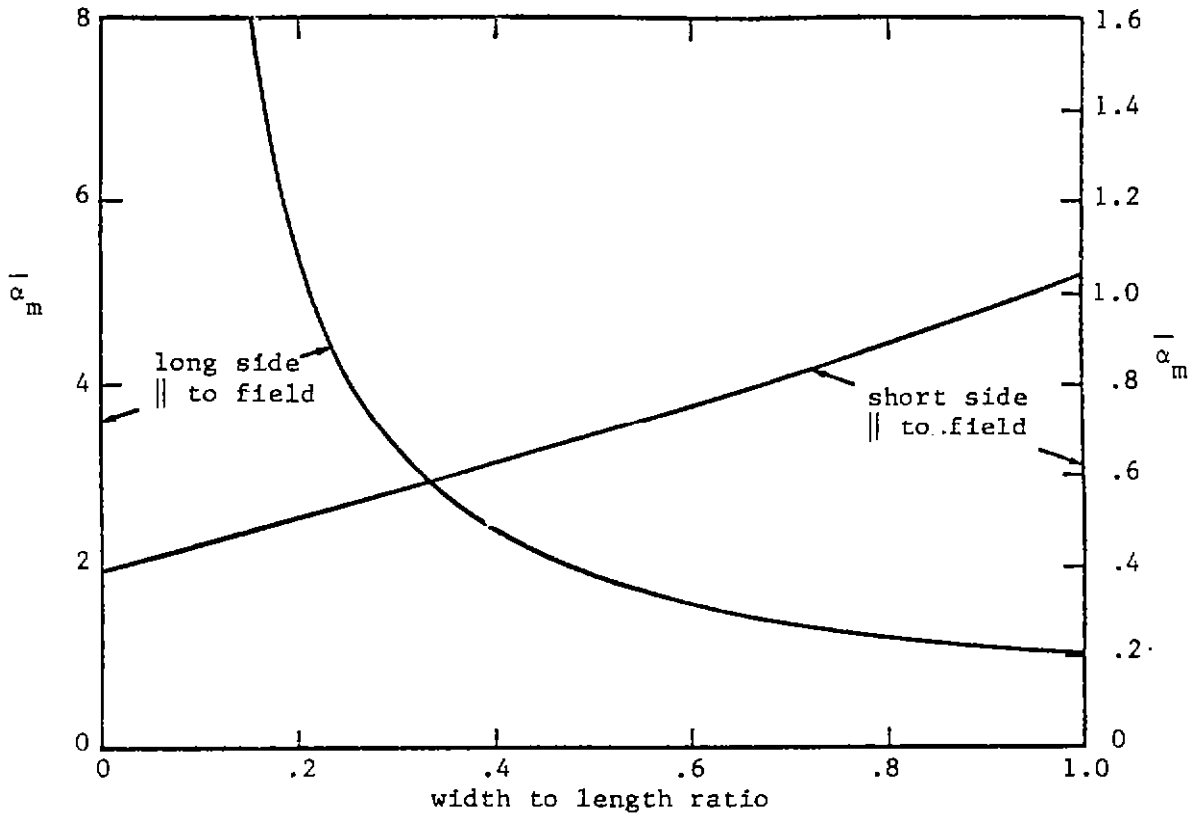

Figure 8a. $\bar{\alpha}_m$ for rectangles.

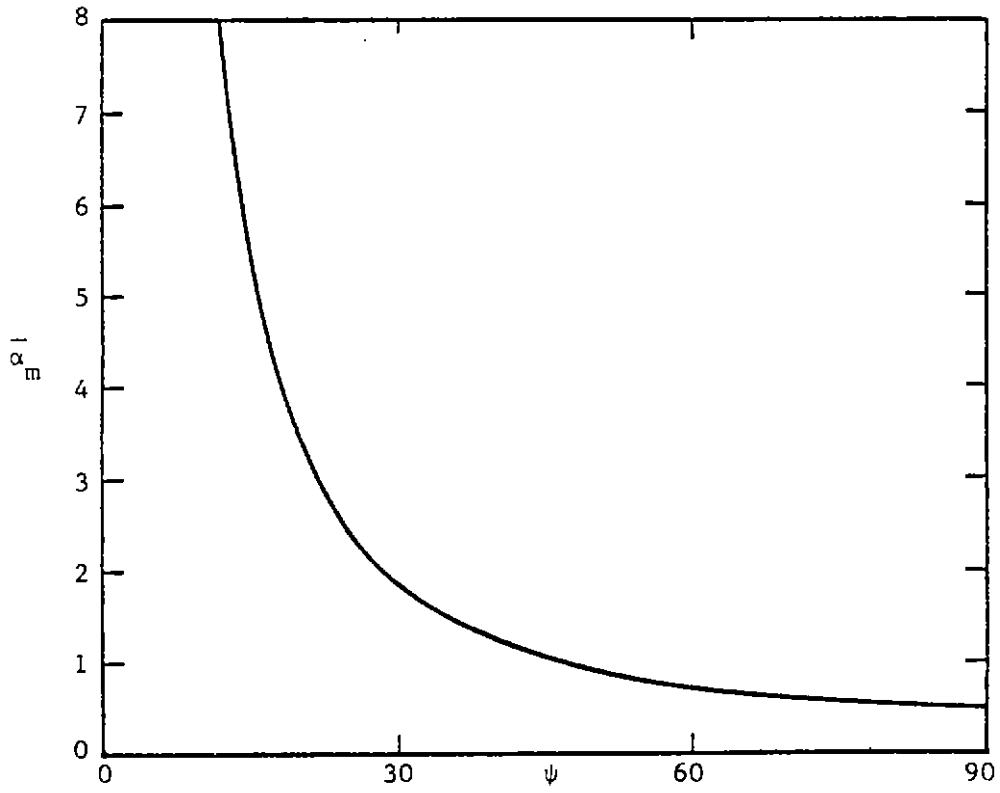

Figure 8b. $\bar{\alpha}_m$ for diamonds.

$$\nabla^2\phi_T = 0$$

$$\phi_T \to z, \qquad z \to \infty$$

$$\phi_T \to 0, \qquad z \to -\infty$$

$$\phi_T = 0 \qquad z = 0, \text{ outside the hole}$$

ϕ_T and $(\partial\phi_T/\partial z)$ continuous through the hole, and then calculating the integral over the aperture, A,

$$\alpha_e = -\int_A \phi_T dS. \tag{6.12}$$

Now, by writing

$$\phi_T = z - \phi(x,y,z) \qquad z > 0 \tag{6.13}$$

$$= -\phi(x,y,-z) \qquad z < 0 \tag{6.14}$$

one sees that all the conditions on ϕ_T are satisfied if

$$\nabla^2\phi = 0 \qquad z > 0$$

$$\phi \to 0 \qquad z \to \infty$$

$$\phi(x,y,0) = 0 \qquad \text{outside the hole}$$

$$\frac{\partial\phi}{\partial z}(x,y,0) = \frac{1}{2} \qquad \text{in hole.}$$

Since $\phi \to 0$ as $z \to \infty$, one can again invoke Green's theorem with an appropriate Green's function and write, anywhere above the x-y plane,

$$\phi(x,y,z) = \frac{1}{2\pi}\int_A \frac{\partial}{\partial z'}\frac{1}{|\underline{r}-\underline{r}'|}\phi(x',y',0)dS'. \tag{6.15}$$

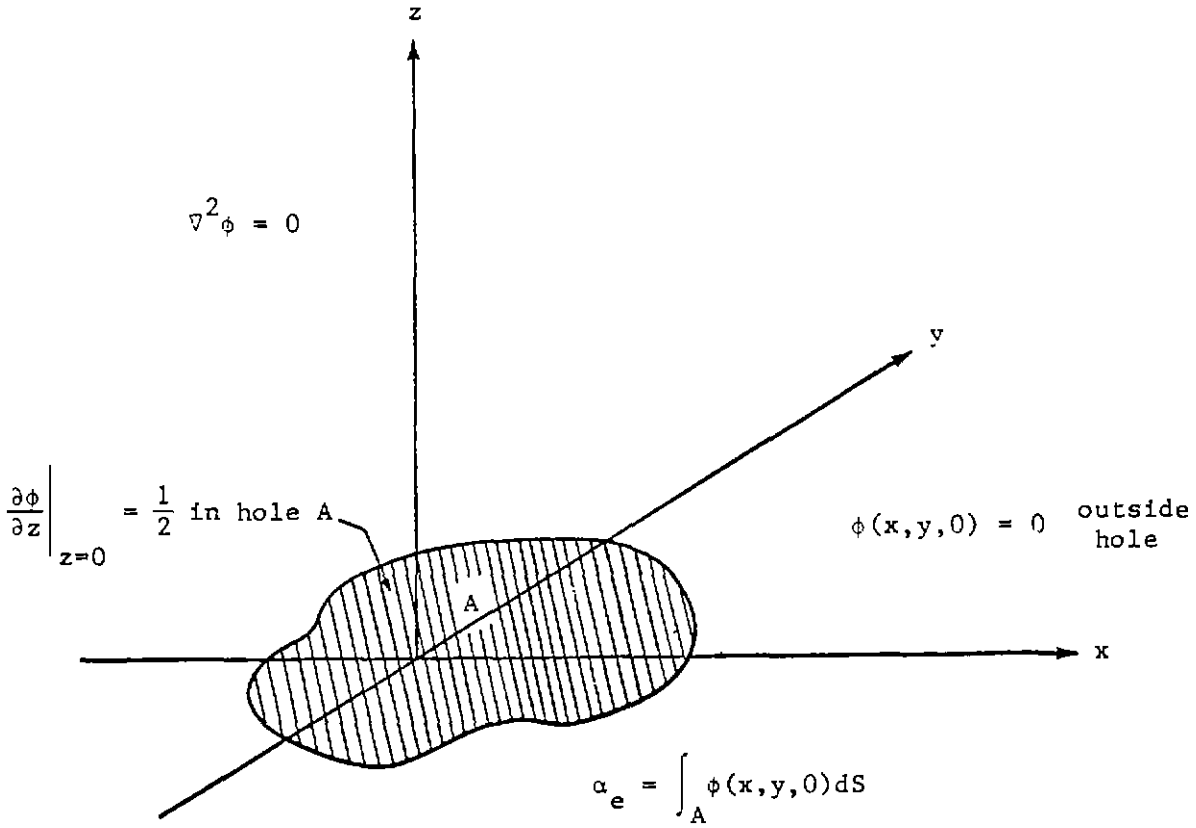

Figure 9. Boundary-value problem for determination of $\bar{\alpha}_e$.

Thus, from the condition on $(\partial\phi/\partial z)$ in the hole,

$$1 = \lim_{z\to 0} \frac{\partial}{\partial z} \frac{1}{\pi} \int_A \frac{\partial}{\partial z'} \frac{1}{|\underline{r}-\underline{r}'|} \phi(x',y',0)dS' \tag{6.16}$$

This is not a real integral equation for ϕ in the aperture since, if one tries to take the derivative inside the integral, divergent integrals would arise. Nevertheless, equation (6.16) can be used as it stands if one is interested in a numerical solution. The unknown function, ϕ, is assumed constant on several small rectangular zones making up the aperture A, and the required integral, derivative, and limit can be performed analytically for a rectangular zone. One thus arrives at a matrix equation that is quite well conditioned, even though equation (6.16) may appear not very promising for numerical work. Once ϕ has been determined in the aperture, the normalized basic polarizability can be found by numerically evaluating the expression

$$\bar{\alpha}_e = \frac{P_h}{A^2} \int_A \phi(x,y,0)dxdy \tag{6.17}$$

The above procedure was used to determine the $\bar{\alpha}_e$ for rectangles and diamonds, and the results are given in table 2 and figure 10. In addition, a procedure to extrapolate the numerical results to an infinite number of zones in the aperture was used. We have already discussed this procedure in connection with the determination of $\bar{\alpha}_m$.

An interesting mathematical puzzle arose during this work on basic electric polarizabilities. Because equation (6.16) looks a little sick for numerical work, it was decided to use the method described above for the simplest possible aperture, the infinite slit, as a test case. It is not difficult to show that, for zones of equal width, the matrix equation for the N-zone approximation to equation (6.16) for the slit problem is just

$$\frac{8}{\pi} \sum_{j=1}^{N} \frac{N\phi_j}{1-4(i-j)^2} = 1 \qquad i = 1, 2, \ldots N \tag{6.18}$$

and the N-zone approximation to $\bar{\alpha}_e$ is given by

$$\bar{\alpha}_e(N) = \frac{2}{N} \sum_{j=1}^{N} \phi_j, \tag{6.19}$$

Table 2a

$\bar{\alpha}_e$ for rectangles

width to length ratio	$\bar{\alpha}_e$
.00	$\pi/8$ = .393
.05	.402
.10	.410
.15	.417
.20	.423
.25	.428
.30	.433
.35	.437
.40	.440
.45	.443
.50	.446
.55	.448
.60	.450
.65	.451
.70	.452
.75	.453
.80	.454
.85	.454
.90	.455
.95	.455
1.00	.455

Table 2b

$\bar{\alpha}_e$ for diamonds

ψ, ½ angle of pointier vertices (degrees)	$\bar{\alpha}_e$
0	$\pi/6$ = .524
5	.516
10	.504
15	.492
20	.481
25	.472
30	.464
35	.459
40	.456
45	.455

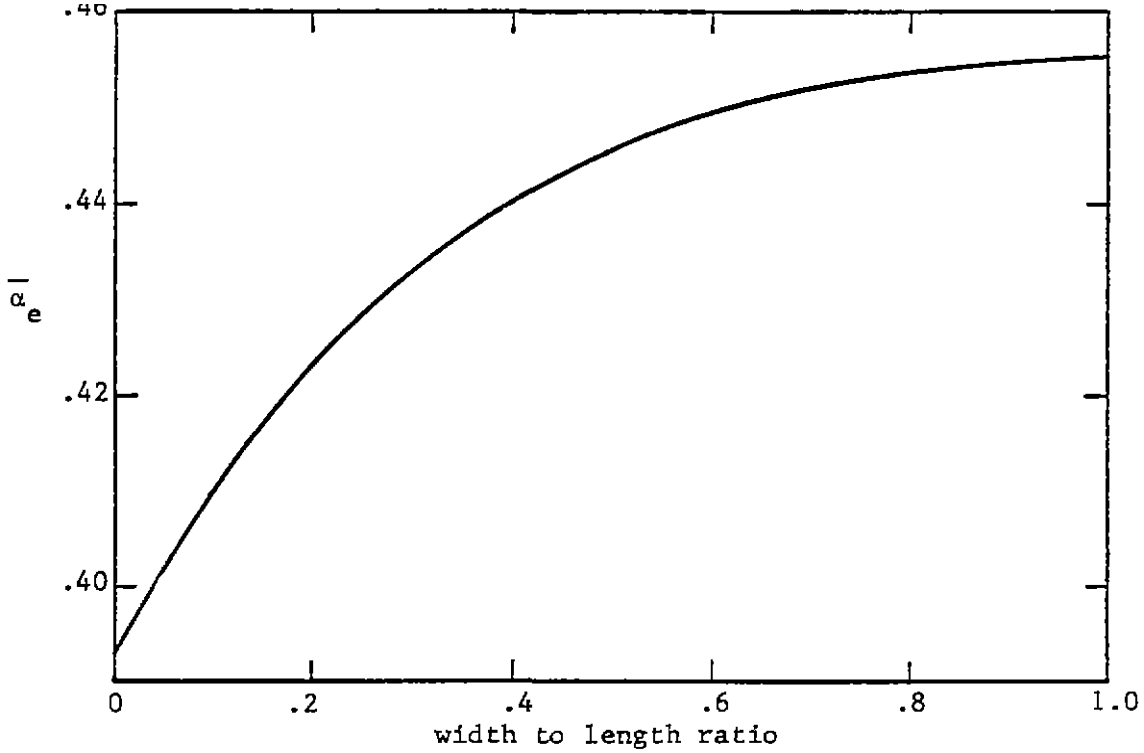

Figure 10a. $\bar{\alpha}_e$ for rectangles.

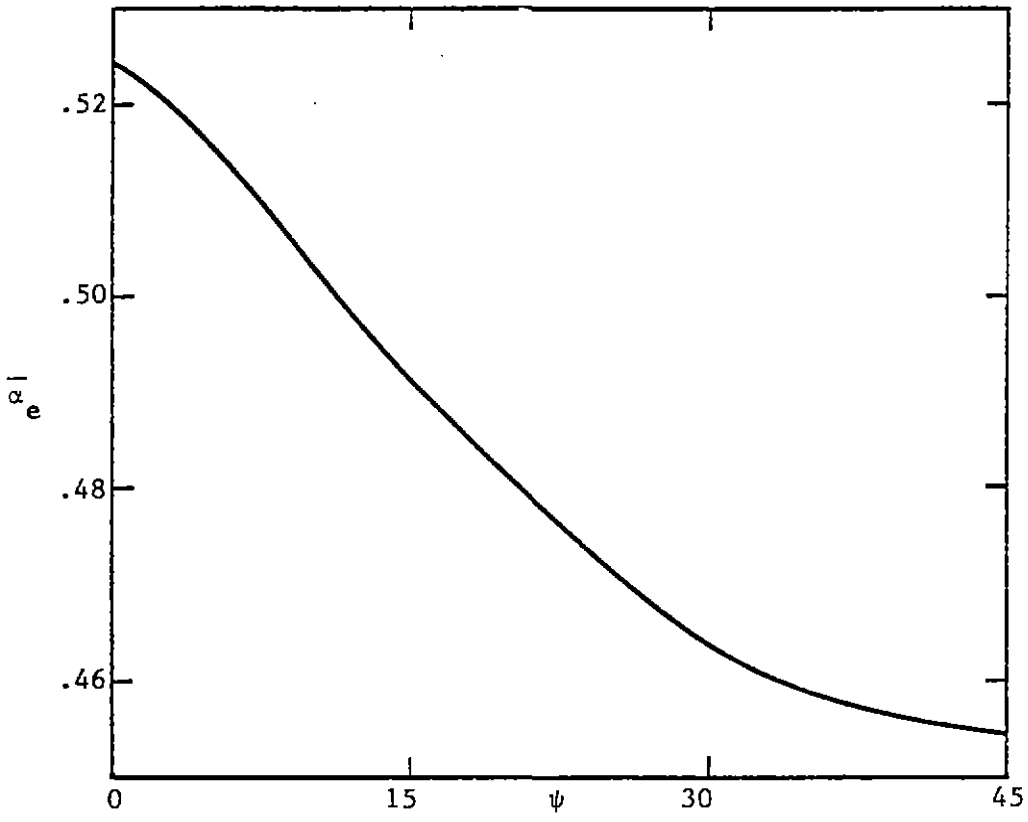

Figure 10b. $\bar{\alpha}_e$ for diamonds.

the ϕ_j being determined by solving equations (6.18). Now, from the analytical solution of the slit problem, $\bar{\alpha}_e(\infty)$ is just $\pi/8$, so defining

$$x_j \equiv (8/\pi)\phi_j,$$

equations (6.18) and (6.19) can be rewritten as

$$\sum_{j=1}^{N} \frac{x_j}{1-4(i-j)^2} = \frac{1}{N} \qquad i = 1, 2, \ldots N \tag{6.20}$$

and

$$r \equiv \frac{\bar{\alpha}_e(N)}{\bar{\alpha}_e(\infty)} = \frac{2}{N} \sum_{j=1}^{N} x_j \tag{6.21}$$

The interesting thing is that the numerical result is just

$$r = \frac{N+1}{N} \tag{6.22}$$

This is true to 12 figure accuracy for any N between one and twenty. Therefore an analytical proof of equation (6.22) was attempted. However, up to now, no satisfactory proof has been found, and so the analytical proof of equation (6.22) from equations (6.20) and (6.21) is a puzzle left to the interested reader.

From the tables and curves of this section it is apparent that, with the normalization we have chosen, $\bar{\alpha}_e$ is roughly the same for almost any reasonably shaped hole, namely around .4 or .5. This, of course, is the reason we chose this normalization in the first place. A further example is the elliptical hole, for which

$$\bar{\alpha}_e = \frac{4}{3\pi} = .424$$

independent of the eccentricity of the ellipse.

VII. Effect of a Nearby Conductor on Hole Polarizabilities

In Section VI we presented ways to calculate the basic polarizabilities of a hole, i.e., the polarizabilities of a hole of the same shape that is all by itself in an infinite plane with no other conductors to look at. In this section we wish to study how a hole's polarizabilities get altered by the presence of a nearby conductor.

To study the effect of a nearby conductor, we will solve exactly a particular boundary-value problem where the proximity of a nearby conductor to the hole is the single parameter of interest. A sketch of the problem to be solved is given as figure 11. An infinite plane contains a circular hole of radius a. A parallel infinite plane is a distance h away. Far away from the plane with a hole there exists a uniform electric field, E_o, pointing in the negative z direction. With the two planes at zero potential, the normalized electric polarizability of the hole is given by

$$\bar{\alpha}_e = \frac{P_h}{E_o A^2} \int_A \phi(x,y,h)dS$$

$$= \frac{2}{E_o \pi a^3} \int_A \phi(x,y,h)dS \qquad (7.1)$$

where ϕ is the electrostatic potential of the field and the integral is over the circular hole, A.

There are several reasons for our choice of this particular configuration to study the effect of nearby conductors. Some of these reasons are:

1. There is basically only one parameter of the problem; $\bar{\alpha}_e$ is a function of a/h only.
2. It is possible that the geometrical configuration to be studied could have a practical application as an electric field sensor in a ground plane.
3. As will be shown shortly, $\bar{\alpha}_e$ and $\bar{\alpha}_m$ are simply related. This fact reduces the amount of calculation and data presentation to a minimum.
4. The two asymptotic forms of $\bar{\alpha}_e$ as a function of a/h are simply determined from physical arguments. These asymptotic forms are of interest in

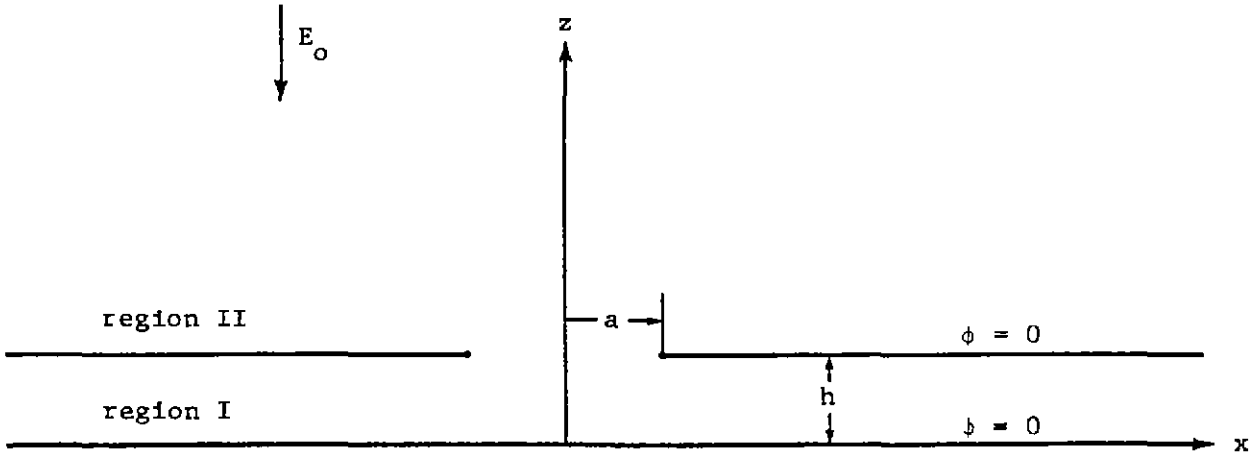

a. cross-sectional view.

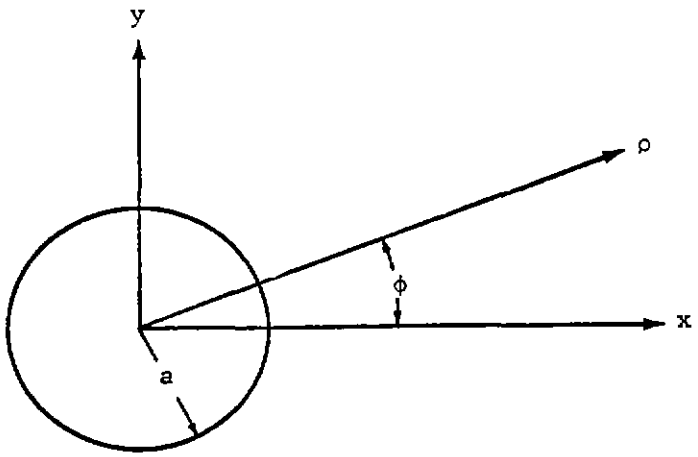

b. top view

Figure 11. A circular hole in a plane above another plane.

themselves and also as a check on the numerical work.

5. Perhaps most important, the problem can be reduced by well known techniques to the solution of a well behaved, one-dimensional, integral equation, just what is needed from the numerical computation point of view.

There is nothing further to say about the first point above. We will discuss the second, third, and fourth points in order before we turn to the exact solution of the problem.

If one looks at the configuration of figure 11 as an electric field sensor, the electrostatic quantities to be calculated are the equivalent area (the charge induced on the bottom plate divided by $\varepsilon_o E_o$ when the two plates are at the same potential) and the difference in the capacity between the two plates when the hole is closed and the capacity between the two plates when the hole is open. By applications of Green's theorem similar to that in Section III, it can readily be shown that the normalized equivalent area, A, is given by

$$\overline{A} \equiv Q/(\pi a^2 \varepsilon_o E_o) = (a/2h)\overline{\alpha}_e$$

and that the change in capacitance is given by

$$(C_{closed} - C_{open}) \frac{h}{\varepsilon_o \pi a^2} = (a/2h)\overline{\alpha}_e = \overline{A}.$$

In order to determine the relation between $\overline{\alpha}_e$ and $\overline{\alpha}_m$ for the configuration of figure 11, let us consider the solution of the electrostatic problem through the use of the electric vector potential, $\underline{A}^e$. The symmetry of the problem tells us that we need only the A_ϕ^e component of vector potential, i.e.,

$$E_z = \frac{1}{\rho} \frac{\partial}{\partial \rho} \rho A_\phi^e$$

$$E_\rho = - \frac{\partial A_\phi^e}{\partial z} .$$

Thus we have

$$\bar{\alpha}_e = \frac{4}{a^2}\int_o^a \phi(\rho)\rho d\rho$$

$$= \frac{4}{E_o a^2}\int_o^a\int_\rho^a E_\rho(\rho')d\rho'\rho d\rho$$

$$= \frac{-4}{E_o a^2}\int_o^a\int_\rho^a \frac{\partial A_\phi^e(\rho')}{\partial z}\, d\rho'\rho d\rho$$

$$= \frac{-4}{E_o a^2}\int_o^a \frac{\partial A_\phi^e(\rho')}{\partial z}\, d\rho' \int_o^{\rho'} \rho d\rho$$

$$= \frac{-2}{E_o a^2}\int_o^a \rho^2 \frac{\partial A^e(\rho)}{\partial z}\, d\rho \qquad (7.2)$$

while A_ϕ^e is determined from the solution of the boundary value problem:

$$\nabla^2 A_\phi^e - (A_\phi^e/\rho^2) = 0 \qquad \text{in regions I and II}$$

$$\frac{\partial A_\phi^e}{\partial z} = 0 \qquad (z = h,\ \rho > a;\ \text{and } z = 0)$$

$$A_\phi^e \to -\frac{E_o\rho}{2} \qquad z \to \infty$$

Now if one calculates $\bar{\alpha}_m$ by using the magnetic scalar potential Ω, and writes $\Omega = \cos\phi f(\rho,z)$, the boundary value problem determining $f(\rho,z)$ is easily seen to be (the external field is assumed to be $\Omega_o = H_o x = H_o\rho\cos\phi$)

$$\nabla^2 f - \frac{f}{\rho^2} = 0 \qquad \text{in regions I and II}$$

$$\frac{\partial f}{\partial z} = 0 \qquad (z = h,\ \rho > a;\ \text{and } z = 0)$$

$$f \to H_o\rho \qquad z \to \infty$$

By comparing the two boundary-value problems, it is clear that

$$f = -\frac{2H_o}{E_o} A_\phi^e \tag{7.3}$$

Now, by definition,

$$\bar{\alpha}_m = \frac{P_h}{H_o A^2} \int_A x \frac{\partial f}{\partial z} \cos \phi dS$$

$$= \frac{2}{H_o d^2} \int_o^a \rho^2 \frac{\partial f}{\partial z} d\rho . \tag{7.4}$$

Thus, by substituting equation (7.3) into equation (7.4) and comparing with equation (7.2), it becomes obvious that

$$\bar{\alpha}_m = 2\bar{\alpha}_e \tag{7.5}$$

This relation is well known for a circular hole in an isolated plane. The fact that it is still rigorously true if there is a nearby parallel plane is perhaps not so well known, but it is one reason for our choice of this particular boundary-value problem; the data presentation is minimized. We will make no further use of A_ϕ^e or Ω in this section. They have been invoked solely as a way of proving equation (7.5).

The asymptotic form of $\bar{\alpha}_e$ as h/a approaches zero is easily determined from the basic formula, (7.1). As h/a approaches zero, the potential over most of the hole will be just hE_o since the potential is zero at the bottom plate and the field will be equal to the external field over most of the region $\rho < a$. Thus

$$\bar{\alpha}_e \to \frac{P_h}{E_o A^2} \cdot hE_o A = \frac{hP_h}{A} \tag{7.6}$$

or, for our circular hole,

$$\bar{\alpha}_e \to 2h/a \tag{7.7}$$

The determination of the asymptotic form of $\bar{\alpha}_e$ as h/a gets large requires

a little more algebra, but it is still straightforward. The effective dipole moment induced in the hole approaches the effective dipole moment induced in a hole in an isolated plane by a modified electric field. This modified electric field is the difference between the external electric field and the electric field on the bottom of the upper plane with the hole closed but with all the image dipoles present. These image dipoles are due to the presence of the second plane, and they are at positions $\rho = 0$; $z = \pm 2nh$, all positive n. If one removes the second plane the strengths of the image dipoles must be set equal to $2p_{eff}$, where p_{eff} is the effective electric dipole moment in the hole. This is because p_{eff} is the dipole moment to be used in conjunction with the exact Green's function for region I; if we wish to calculate the field of the image dipoles we really have to include a pair of effective dipoles at each image position. Thus, if the polarizability of the isolated hole is equal to α_o, we have

$$p_{eff} = \varepsilon_o \alpha_o \left\{ E_o - 2(2p_{eff}) \cdot \frac{2}{4\pi\varepsilon_o} \sum_{n=1}^{\infty} \frac{1}{(2nh)^3} \right\}$$

i.e.

$$p_{eff} = \frac{\varepsilon_o \alpha_o E_o}{1+(\alpha_o/4\pi h^3) \sum_{n=1}^{\infty} (1/n^3)}$$

This gives a normalized electric polarizability of

$$\bar{\alpha}_e = \frac{(P_h/A^2)\alpha_o}{1+(\alpha_o/h^3)(\zeta(3)/4\pi)} \tag{7.8}$$

where $\zeta(z)$ is the Riemann-Zeta function [8]. Equation (7.6) and (7.8) are the asymptotic forms for any hole shape. For our circular hole, $\alpha_o = (2/3)a^3$, and thus equation (7.8) can be reduced to

$$\bar{\alpha}_e = \frac{4/3\pi}{1+(a/h)^3(\zeta(3)/6\pi)} \tag{7.9}$$

Let us now turn to the exact solution of our boundary-value problem, i.e. to the formulation of a well behaved, one-dimensional, integral equation whose numerical solution will give us the quantity we want to know, $\bar{\alpha}_e$.

Above the $z = h$ plane of figure 11 we can write the electrostatic potential, ϕ, as

$$\phi = (z - h)E_o + \int_o^\infty f(\alpha)J_o(\alpha\rho)e^{-\alpha|z-h|}\, d\alpha,$$

while between $z = 0$ and $z = h$ we can write

$$\phi = \int_o^\infty f(\alpha)\, \frac{\sinh \alpha z}{\sinh \alpha h}\, J_o(\alpha\rho)d\alpha.$$

Thus, from the facts that $\phi = 0$ on $(z = h,\ \rho > a)$ and $\partial\phi/\partial z$ is continuous on $(z = h,\ \rho < a)$ we have

$$\int_o^\infty f(\alpha)J_o(\alpha\rho)d\alpha = 0 \qquad \rho > a$$

and

$$\int_o^\infty \alpha f(\alpha)\{\coth(\alpha h) + 1\}J_o(\alpha\rho)d\alpha = E_o, \qquad \rho < a$$

or, using a as the unit of length by setting $\alpha a = u$, $\rho/a = \rho'$, and $h/a = d$,

$$\int_o^\infty f(u)J_o(u\rho')du = 0 \qquad \rho' > 1$$

$$\int_o^\infty uf(u)\left\{1 + \frac{\coth(ud)-1}{2}\right\} J_o(u\rho')du = \frac{E_o a^2}{2} \qquad \rho' < 1.$$

But from reference 9 (pp. 108-109, equations 4.6.17 and 4.6.18), the solution of the above pair of dual integral equations is

$$f(u) = \frac{2}{\sqrt{\pi}} \int_o^1 h_1(x)\sin(ux)dx \tag{7.10}$$

where $h_1(x)$ is the solution of

$$h_1(x) + \int_o^1 K(x,u)h_1(u)du = H(x). \tag{7.11}$$

In equation (7.11) $K(x,u)$ is given by

$$K(x,u) = \frac{1}{\pi}\int_0^\infty \{\cos(|x-u|t) - \cos(|x+u|t)\}\,\frac{\coth(td)-1}{2}\,dt$$

$$= -\frac{-1}{2\pi d}\sum_{n=1}^{\infty}\left\{\frac{(x-u)^2}{n[(2nd)^2+(x-u)^2]} - \frac{(x+u)^2}{n[(2nd)^2+(x+u)^2]}\right\} \qquad (7.12)$$

and H(x) is given by

$$H(x) = \frac{1}{\sqrt{\pi}}\int_0^x \frac{u(E_o a^2/2)}{(x^2-u^2)^{\frac{1}{2}}}\,du$$

$$= \frac{E_o a^2 x}{2\sqrt{\pi}} \qquad (7.13)$$

From equations (7.11) through (7.13) the integral equation for h(x) (defined as $E_o a^2 h_1(x)/2\pi^{3/2}$) may be written

$$h(x) - \frac{1}{2\pi d}\int_{-1}^{1}\sum_{n=1}^{\infty}\frac{(x-u)^2}{n[(2nd)^2+(x-u)^2]}\,h(u)du = x \qquad (7.14)$$

From equation (7.1) the quantity we wish to calculate is

$$\bar{\alpha}_e = \frac{4}{E_o a^3}\int_0^a \phi(\rho)\rho\,d\rho$$

$$= \frac{4}{E_o a^3}\int_0^a \rho\int_0^\infty f(\alpha)J_o(\alpha\rho)\,d\alpha\,d\rho. \qquad (7.15)$$

But by substituting from equation (7.10), interchanging orders of integration, and performing the two inner integrals, equation (7.15) reduces to

$$\bar{\alpha}_e = \frac{4}{\pi}\int_0^1 x h(x)\,dx \qquad (7.16)$$

The boundary-value problem has now been reduced to the determination of h(x) from equation (7.14) and the subsequent calculation of $\bar{\alpha}_e$ from equation (7.16). Such operations are ideally suited to numerical methods. The results of the numerical work are presented in table 3 and figure 12.

Table 3

$\bar{\alpha}_e$ for hole of figure 11

h/a	$\bar{\alpha}_e$	$3\pi\bar{\alpha}_e/4$	eq. (7.18)	a/h	$\bar{\alpha}_e$	$3\pi\bar{\alpha}_e/4$	eq. (7.18)
.00	0	0	0	.00	.4244	1.0000	.4244
.05	.0840	.1979	.0802	.05	.4244	1.0000	.4244
.10	.1490	.3511	.1439	.10	.4244	1.0000	.4244
.15	.1997	.4705	.1946	.15	.4243	.9997	.4243
.20	.2381	.5610	.2350	.20	.4242	.9995	.4242
.25	.2689	.6336	.2673	.25	.4240	.9990	.4240
.30	.2943	.6934	.2934	.30	.4237	.9983	.4237
.35	.3151	.7424	.3145	.35	.4233	.9974	.4233
.40	.3320	.7823	.3317	.40	.4228	.9962	.4228
.45	.3459	.8150	.3457	.45	.4222	.9948	.4222
.50	.3574	.8421	.3573	.50	.4214	.9929	.4214
.55	.3669	.8645	.3669	.55	.4205	.9908	.4205
.60	.3749	.8833	.3749	.60	.4195	.9884	.4195
.65	.3815	.8989	.3815	.65	.4184	.9858	.4184
.70	.3871	.9121	.3871	.70	.4171	.9828	.4171
.75	.3919	.9234	.3919	.75	.4157	.9795	.4157
.80	.3959	.9328	.3959	.80	.4141	.9757	.4141
.85	.3993	.9408	.3993	.85	.4125	.9719	.4125
.90	.4022	.9477	.4022	.90	.4107	.9677	.4107
.95	.4047	.9536	.4047	.95	.4088	.9632	.4088
1.00	.4069	.9587	.4069	1.00	.4069	.9587	.4069

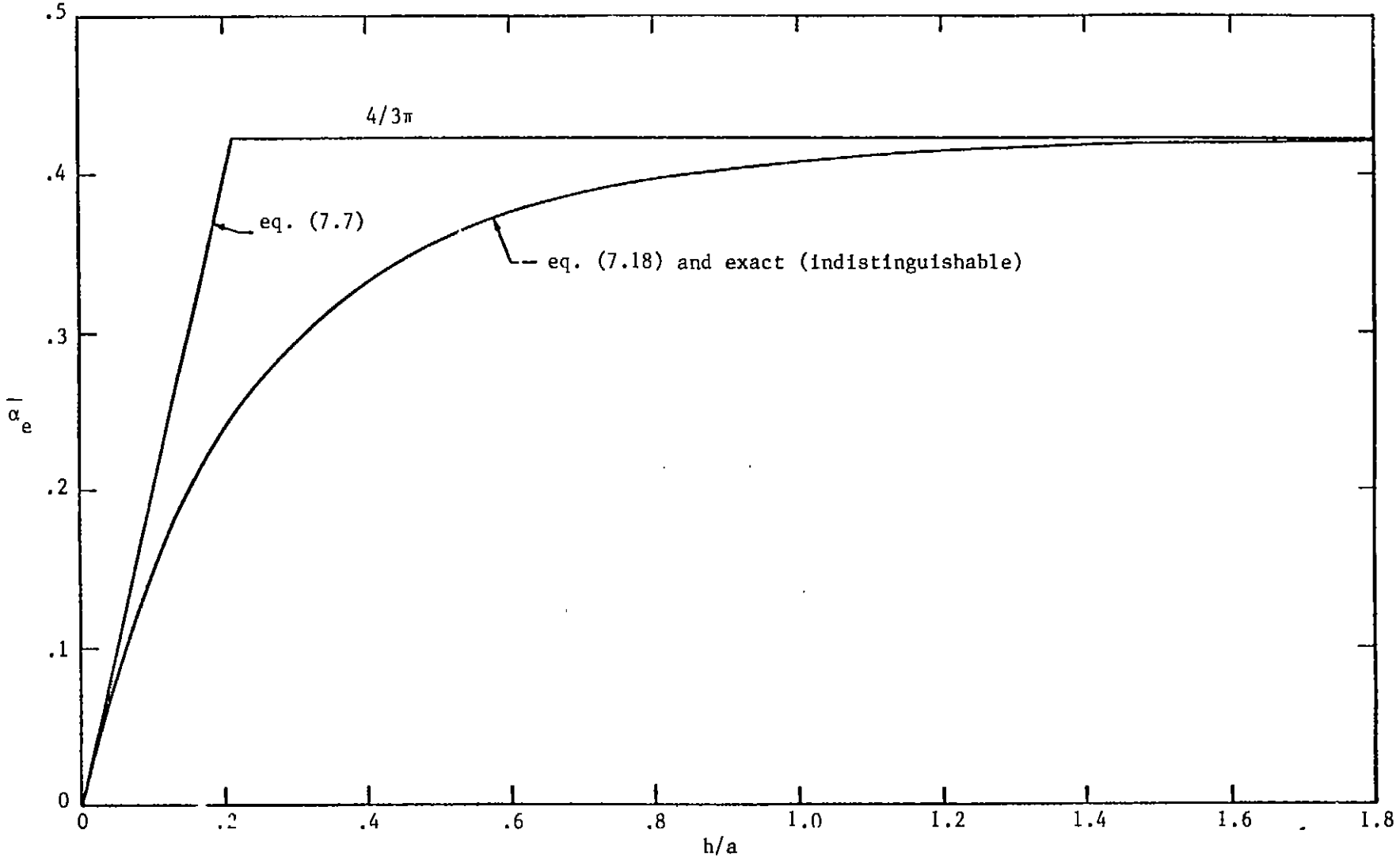

Figure 12. Normalized electric polarizability of the hole of figure 11.

Also drawn on figure 12 is the value of $\bar{\alpha}_e$ derived from the variational expression based on equations (7.14) and (7.16),

$$\bar{\alpha}_e \simeq \frac{\pi}{2}\left[\frac{2}{\pi}\int_{-1}^{1} xh(x)dx\right]^2 \left\{\int_{-1}^{1} h^2(x)dx - \frac{1}{2\pi d}\int_{-1}^{1}\sum_{n=1}^{\infty}\frac{h(t)(x-t)^2h(x)}{n[(2nd)^2+(x-t)^2]}dxdt\right\}^{-1} \qquad (7.17)$$

by substituting $h(x) = x$. This substitution allows the required integrations to be performed and reduces the variational estimate of $\bar{\alpha}_e$ to

$$\bar{\alpha}_e \approx \frac{4/3\pi}{1+(2/\pi)\sum_{n=1}^{\infty} F(nd)} \qquad (7.18)$$

where

$$F(x) = \tan^{-1}\left(\frac{1}{x}\right) + x - \left(x^3 + \frac{3x}{2}\right)\ln\left(1 + \frac{1}{x^2}\right)$$

The trial function, x, is the exact solution of (7.14) as d approaches ∞, so of course equation (6.18) reduces to equation (7.9) as d gets large.

We note that as d approaches zero the variational expression for $\bar{\alpha}_e$ approaches

$$\bar{\alpha}_e \to \frac{2d}{3\int_o^{\infty} F(x)dx} = \frac{16d}{9},$$

which differs from the true asymptotic value, equation (7.7), by only 11%. Since this is a worst case for our trial function, the variational value never differs from the correct value by more than 11%. For $d > .5$, the variational value differs from the correct value by less than .03%.

From the table or curve we can see that $\bar{\alpha}_e$ differs from its asymptotic value by less than 5% as long as h is greater than a. This allows one to say with some confidence that the effect of nearby conductors (i.e., the cables that are being shielded) on the polarizabilities of holes is negligible for most cable shielding applications.

VII. Effect of Surface Curvature on Hole Polarizabilities

We will study the effect of surface curvature on the polarizabilities of a hole by calculating the normalized polarizabilities of a long slit in a hollow, circular, cylindrical shell, as shown in figure 13, and comparing these polarizabilities with those of a slit of the same width located in an infinite plane. The difference will give us an indication of the error introduced by using the basic polarizabilities of Section VI even though the hole is located in a curved surface. The reasons for picking this particular problem for solution are:

1. There is only one parameter of the problem; $\bar{\alpha}_e$ and $\bar{\alpha}_m$ are functions of d/a only. Since d/a is a measure of the hole size relative to the radius of curvature of the surface, the curvature effect seems to be fairly well isolated.
2. As will be shown, $\bar{\alpha}_e$ and $\bar{\alpha}_m$ are equal. The necessary data presentation is therefore quite small.
3. Assuming the slit to be infinitely long, the boundary-value problem can be solved exactly.

There is nothing further to be said about the first point above. We will give a brief proof of the equality of the two polarizabilities, mentioned in the second statement, before going on to the explicit calculation of $\bar{\alpha}_e$.

Consider a perfectly conducting, hollow, slit cylinder of some arbitrary cross-section, such as is shown in figure 14. Define a line t, of length d, that makes the cross-section a closed loop. The normalized electric polarizability of a length ℓ of the strip is given, from the basic definition, by

$$\bar{\alpha}_e = -\frac{P_h}{\varepsilon_o A^2}\int_o^{\ell}\int_o^{d}\phi(s,z)\,ds\,dz$$

where the origin of the s coordinate is indicated in figure 14. Thus, since ϕ is independent of z,

$$\bar{\alpha}_e = -\frac{2\ell}{E_o(\ell d)^2}\cdot \ell\int_o^{d}\phi(s)\,ds$$

$$= -\frac{2}{d^2}\int_o^{d}\frac{\phi(s)}{E_o}\,ds \qquad (8.1)$$

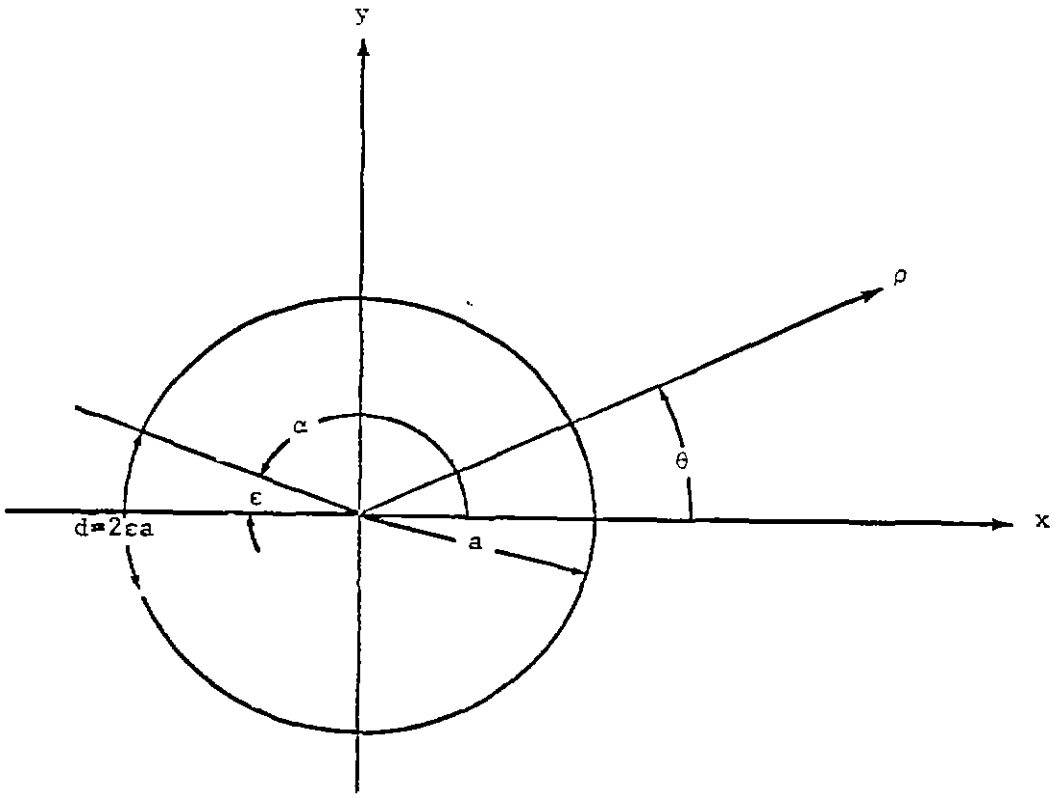

Figure 13. Cross-section of circular cylinder with a slit of angular width 2ε.

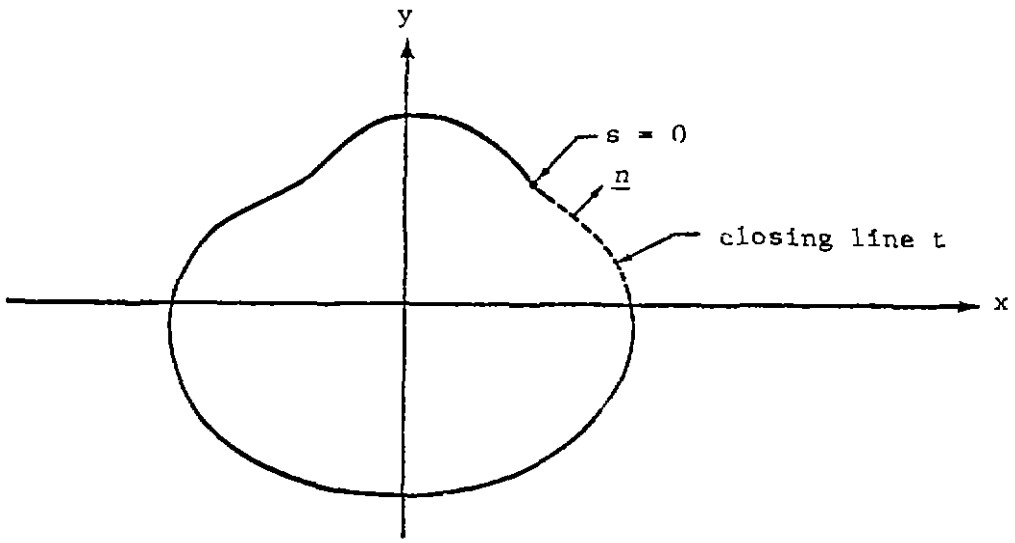

Figure 14. Cross-section of arbitrary cylinder with a slit.

where E_o is the normal E field that would exist at the middle of t if t were closed by perfect conductor and the cylinder bore a charge density Q_o per unit length, and ϕ is the actual potential along t (ϕ is zero on the conducting portion of the cross-section) when the cylinder bears a charge density Q_o per unit length.

Similarly, the normalized magnetic polarizability is given by

$$\bar{\alpha}_m = \frac{2}{d^2} \int_o^d \frac{s}{H_o} \frac{\partial \Omega}{\partial n} \, ds \tag{8.2}$$

where H_o is the tangential H field that would exist at the middle of t if t were closed and the cylinder carried a total current I_o, and Ω is the actual magnetic potential when the cylinder carries a total current $-I_o$. From the definition of the static problems it can be seen that (ϕ/E_o) and (Ω/H_o) are the real and imaginary parts of a single complex potential function. Therefore, from the Cauchy-Riemann relation,

$$\frac{\partial}{\partial s} \frac{\phi(s)}{E_o} = \frac{\partial}{\partial n} \frac{\Omega}{H_o} .$$

Thus

$$\bar{\alpha}_e = - \frac{2}{d^2} \int_o^d \frac{\phi(s)}{E_o} \, ds$$

$$= - \frac{2}{d^2} \frac{s\phi(s)}{E_o} \Bigg|_o^d + \frac{2}{d^2} \int_o^d s \frac{\partial}{\partial s} \frac{\phi(s)}{E_o} \, ds$$

$$= \frac{2}{d^2} \int_o^s s \frac{\partial}{\partial n} \frac{\Omega}{H_o} \, ds$$

$$= \bar{\alpha}_m \tag{8.3}$$

In passing we note that, even for wide slits, the proportionality constant between equivalent voltage and shield current that can be calculated from equation (2.2) is equal to $(\mu_o \varepsilon_o / C_o)$ times the proportionality constant between equivalent current and shield charge that can be calculated from equation (3.2). This

follows from a slight generalization of the above argument demonstrating the equality of $\bar{\alpha}_e$ and $\bar{\alpha}_m$.

Now let us consider the circular cylinder of figure 13 in more detail. If the total charge per unit length on the cylinder is Q_o, the value of E_o to be used in conjunction with equation (8.1) is just

$$E_o = \frac{Q_o}{2\pi\epsilon_o d} . \tag{8.4}$$

By a logarithmic conformal transformation, followed by a transformation given by Smythe ([4], §4.22, eq. 7), it can be shown that the rigorous complex potential of our problem is just

$$\Phi = \phi + i\psi = \frac{Q_o}{4\pi\epsilon_o}\left\{\ln(a/z) - 2i \sin^{-1}\left(\frac{\sin[(i/2)\ln(a/z)]}{\sin(\alpha/2)}\right)\right\} \tag{8.5}$$

where

$$z = x + iy$$

i.e.

$$\ln z = \rho + i\theta .$$

But $\phi(x,y)$, being a solution of Laplace's equation, is equal to its average value over a circle with the point (x,y) as center, as long as the circle encloses no charge. Therefore $\phi(0,0)$ is equal to the average value of ϕ over the inner surface of the cylinder, and since ϕ is zero on the conducting portion of the cylinder,

$$\int_o^d \phi(s)ds = 2\pi d\phi(0,0) \tag{8.6}$$

Thus, from (8.1), (8.4) and (8.5)

$$\bar{\alpha}_e = -\frac{2\pi}{d^2} \lim_{\rho\to 0}\left\{\ln(a/\rho) - 2 \sinh^{-1}\frac{\sinh[\frac{1}{2}\ln(a/\rho)]}{\sin(\alpha/2)}\right\}$$

$$= -4\pi \frac{\ln\cos(d/4a)}{(d/a)^2} . \tag{8.7}$$

We can write equation (8.7) as

$$\bar{\alpha}_e = \bar{\alpha}_{eo} F_c(d/a) \tag{8.8}$$

where

$$F_c(x) = -32 \frac{\ln(\cos x)}{x^2} .$$

In equation (8.8), $\bar{\alpha}_{eo}$ is the limit of $\bar{\alpha}_e$ when d approaches zero ($=\pi/8$), i.e. it is equal to the normalized polarizability of a slit in an infinite plane, what we have called the basic polarizability of the hole. $F_c(d/a)$ is thus a measure of the change in the normalized polarizability of a hole as a function of the ratio of the hole size to the radius of curvature of the surface. The percentage difference of $F_c(x)$ from unity is plotted in figure 15 and given in table 4. For small x it is easy to show that

$$F_c(x) \to 1 + \frac{x^2}{96} . \tag{8.9}$$

Thus the error in hole polarizability due to using the infinite plane polarizability for a small hole in a curved surface is proportional to the square of the ratio of the hole size to the radius of curvature of the surface. It also seems that the proportionality constant is quite small.

We conclude this section by noting that a transformation quite similar to (8.5) can be used to determine the inductive coupling coefficient per unit length for a circular cylindrical shell with N slits of the same width spaced uniformly around its circumference. This quantity, L_s, has been defined for a general cable shield [3]. If c is the optical coverage of the N-slit shield, it turns out that

$$L_s = \frac{\mu_o}{2\pi N} \ln(\sin \frac{\pi c}{2}). \tag{8.10}$$

Furthermore, from the same transformation it follows that

$$S_s = \frac{1}{2\pi N \epsilon_o} \ln(\sin \frac{\pi c}{2}). \tag{8.11}$$

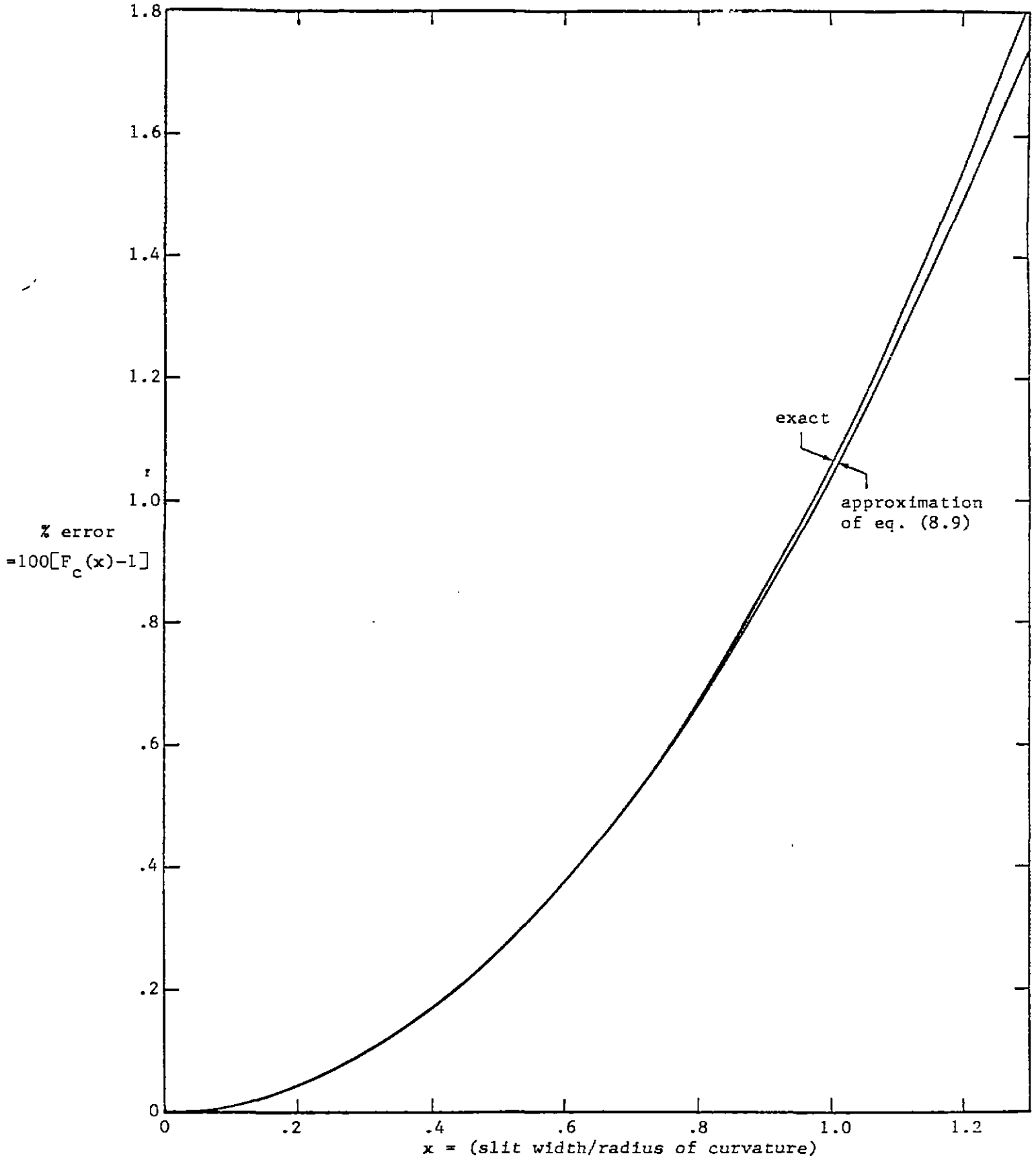

Figure 15. Percent error in $\bar{\alpha}_e$ introduced by surface curvature.

Table 4

x	$100[F_c(x)-1]$	$100(x^2/96)$
.00	.000	.000
.05	.003	.003
.10	.010	.010
.15	.023	.023
.20	.042	.042
.25	.065	.065
.30	.094	.094
.35	.128	.128
.40	.167	.167
.45	.212	.211
.50	.262	.260
.55	.317	.315
.60	.377	.375
.65	.443	.440
.70	.515	.510
.75	.591	.586
.80	.674	.667
.85	.762	.753
.90	.855	.844
.95	.954	.940
1.00	1.059	1.042
1.05	1.170	1.148
1.10	1.286	1.260
1.15	1.409	1.378
1.20	1.537	1.500
1.25	1.671	1.628
1.30	1.812	1.760
1.35	1.958	1.898
1.40	2.111	2.042
1.45	2.270	2.190
1.50	2.436	2.344

IX. Effect of Nearby Holes on Hole Polarizabilities

We will study the effect of nearby holes on hole polarizabilities by examining a particular case of hole interaction that will be directly applicable to our braided shield model. The particular case we will look at is the interaction among the holes forming an infinite diamond lattice in a plane plate as shown in figure 16. This lattice represents an idealization of the lattice of holes in a shield braid. If the hole spacing on the actual shield braid is significantly smaller than the shield diameter, the planar model should give a good approximation of the interaction effect.

The approximations we will make when calculating the polarizability of a hole of the lattice of figure 16 is that we will consider only dipole interactions among the holes and we will assume the dipole fields of all the other holes are uniform over the particular hole we are concentrating on (the hole at the origin).

The polarizabilities of holes, calculated by some method such as that given in Section VI, are proportionality constants between the effective dipole moment induced in the hole and the field (actually the difference in the field on the two sides of the conductor in which the hole is located) that would exist at the position of the hole if the hole were closed. When several holes are present, the field that would exist at the position of a particular hole if that hole were closed must include the fields due to the presence of all the other holes. For easy application to our braided shield model, we would like the proportionality constant between the effective dipole moment induced in a hole and the external field (not including the fields of the other holes). This is the type of proportionality constant one has in mind in the discussions of Section V. The polarizabilities in equations (5.5) and (5.6), for example, are this type of proportionality constant.

To obtain the proportionality constant between the effective magnetic dipole moment and the external field in the x direction, one can make use of the polarizability calculated in Section VI to write, if the holes have lines of symmetry parallel to the x and y axes,

$$m_{eff} = \alpha_m (H_{ext} + H_{int}) \tag{9.1}$$

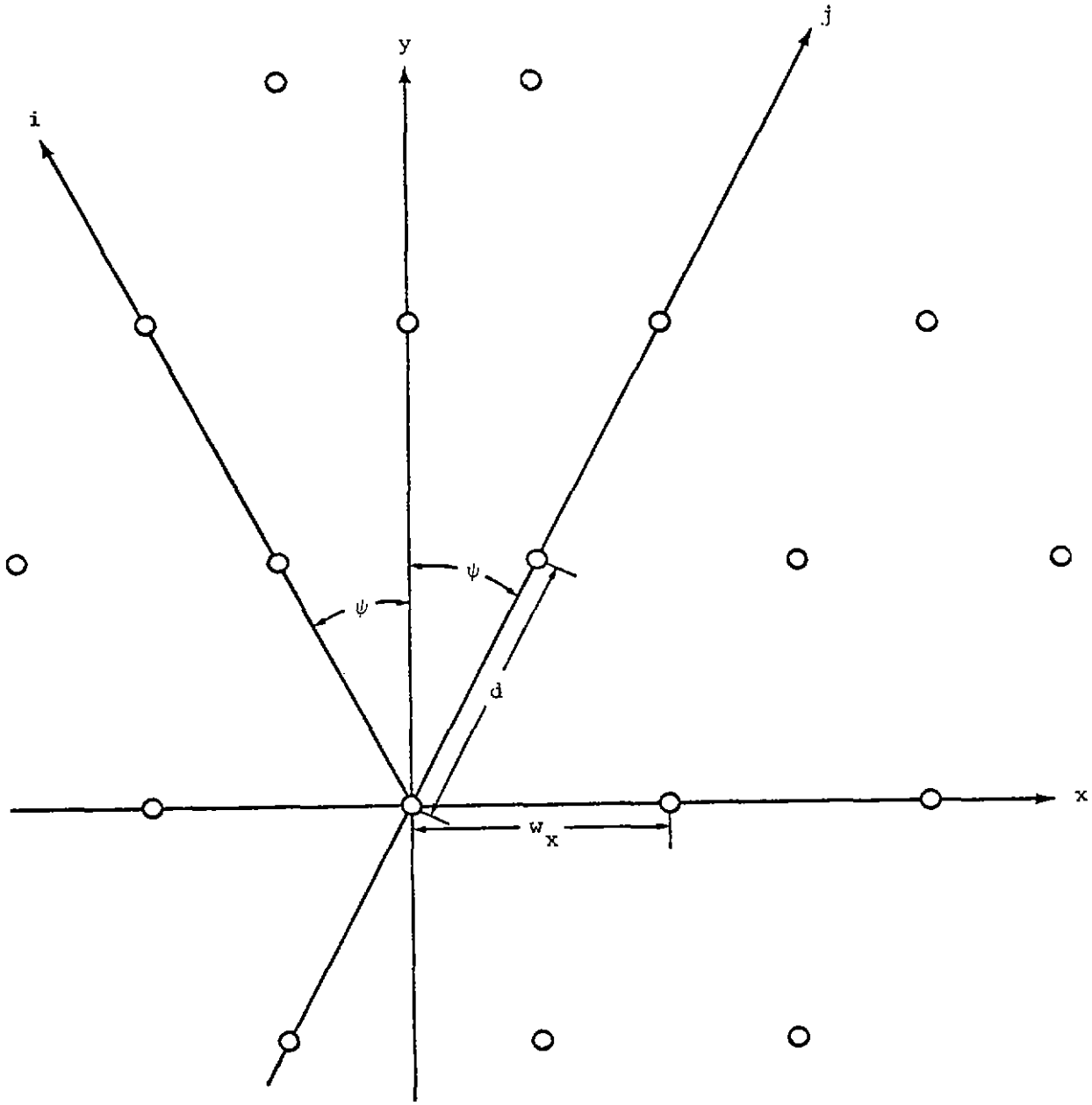

Figure 16. Lattice for dipole interaction sums

where H_{ext} is the external field and H_{int} the jump, through the plate, of the interaction field due to the presence of all the other holes. If we are dealing with an infinite lattice of holes, as in figure 16, all effective dipole moments are the same and we may write, for the hole at the origin,

$$H_{int} = -2 \cdot \frac{1}{2\pi} \cdot m_{eff} \sum_{\substack{i,j=-\infty \\ y\neq 0 \text{ if } i=0}}^{\infty} \left\{ \frac{1}{r_{ij}^3} - \frac{3x_{ij}^2}{r_{ij}^5} \right\} \tag{9.2}$$

where the factor of 2 arises from the fact that equal and opposite fields are induced on the two sides of the plate by each of the other dipoles. In equation (9.2) we have

$$x_{ij} = d(j - i)\sin\psi = (j - i)(w_x/2)$$

$$y_{ij} = d(j + i)\cos\psi = (j + i)(w_x/2)\cot\psi$$

and

$$r_{ij}^2 = x_{ij}^2 + y_{ij}^2 = d^2 (j - i)^2 \sin^2\psi + (j + i)^2 \cos^2\psi$$

$$= d^2(i^2 + j^2 + 2ij \cos 2\psi)$$

$$= \left(\frac{w_x}{2 \sin \psi}\right)^2 (i^2 + j^2 + 2ij \cos 2\psi)$$

Let us define (w_x^3/π) times the sum in equation (9.2) as Σ_h. Then from equations (9.1) and (9.2) we have

$$m_{eff} = \alpha_m \left(H_{ext} - \frac{m_{eff}}{w_x^3} \Sigma_h \right) \tag{9.3}$$

i.e.

$$m_{eff} = \frac{\alpha_m}{1+(\alpha_m/w_x^3)\Sigma_h} H_{ext} \tag{9.4}$$

Thus the polarization constant we desire, between the effective dipole moment of the hole and the external field, which we will denote by $\hat{\alpha}_m$, is given, under our assumptions, by

$$\hat{\alpha}_m = \frac{\alpha_m}{1+(\alpha_m/w_x^3)\Sigma_h} \tag{9.5}$$

where α_m is the polarizability of an isolated hole that can be calculated by the method of Section VI. Since α_m and w_x depend on the particular hole shape and lattice spacing, the significant quantity to tabulate in order to be able to use equation (9.5) is Σ_h. This quantity is a function of ψ only and may be written:

$$\Sigma_h = \frac{16 \sin^3\psi}{\pi} \sum_{i=1}^{\infty} \left\{ \frac{1-3 \sin^2\psi}{i^3} + \sum_{j=-\infty}^{\infty} \frac{(i^2+j^2)(1-3 \sin^2\psi)+2ij(1+\sin^2\psi)}{(i^2+j^2+2ij \cos 2\psi)^{5/2}} \right\} \tag{9.6}$$

In a precisely analogous manner, one can show that $\hat{\alpha}_e$, the proportionality constant between the effective electric dipole moment of a hole and the external electric field is given, for our diamond lattice, by

$$\hat{\alpha}_e = \frac{\alpha_e}{1+(\alpha_e/w_x^3)\Sigma_e} \tag{9.7}$$

where α_e is the electric polarizability of an isolated hole such as would be calculated by the method of Section VI, and

$$\Sigma_e = \frac{16 \sin^3\psi}{\pi} \sum_{i=1}^{\infty} \left\{ \frac{1}{i^3} + \sum_{j=-\infty}^{\infty} \frac{1}{(i^2+j^2+2ij \cos 2\psi)^{3/2}} \right\} \tag{9.8}$$

Table 5 gives values of Σ_h and Σ_e as functions of ψ. We also give, in the table, a column for each of the functions $(\cos^3\psi\Sigma_h)$ and $(\cos^3\psi\Sigma_e)$. These auxiliary functions are well behaved and so may be more suitable for interpolation than Σ_h and Σ_e themselves. These auxiliary functions are also plotted in figure 17.

The practical application of the data calculated in this section may be found in the summarizing discussion of our braided shield model to be presented in the following, final, section.

Table 5

Interaction sums for diamond lattice

ψ(degrees)	Σ_h	$\cos^3\psi\Sigma_h$	Σ_e	$\cos^3\psi\Sigma_e$
0	-1.531	$-(4/\pi)\zeta(3)$=-1.531	$(2/\pi)\zeta(3)$=.765	.765
5	-1.528	-1.511	.829	.820
10	-1.525	-1.456	1.026	.980
15	-1.521	-1.370	1.367	1.232
20	-1.523	-1.264	1.874	1.555
25	-1.566	-1.166	2.578	1.919
30	-1.729	-1.123	3.512	2.281
35	-2.123	-1.167	4.715	2.591
40	-2.861	-1.286	6.232	2.801
45	-4.016	-1.420	8.133	2.875
50	-5.573	-1.480	10.548	2.801
55	-7.378	-1.392	13.733	2.591
60	-9.043	-1.130	18.250	2.281
65	-9.678	- .731	25.424	1.919
70	-6.856	- .274	38.869	1.555
75	8.671	.150	71.042	1.232
80	92.270	.483	187.100	.980
85	1047.330	.693	1238.502	.820
90	∞	.765	∞	.765

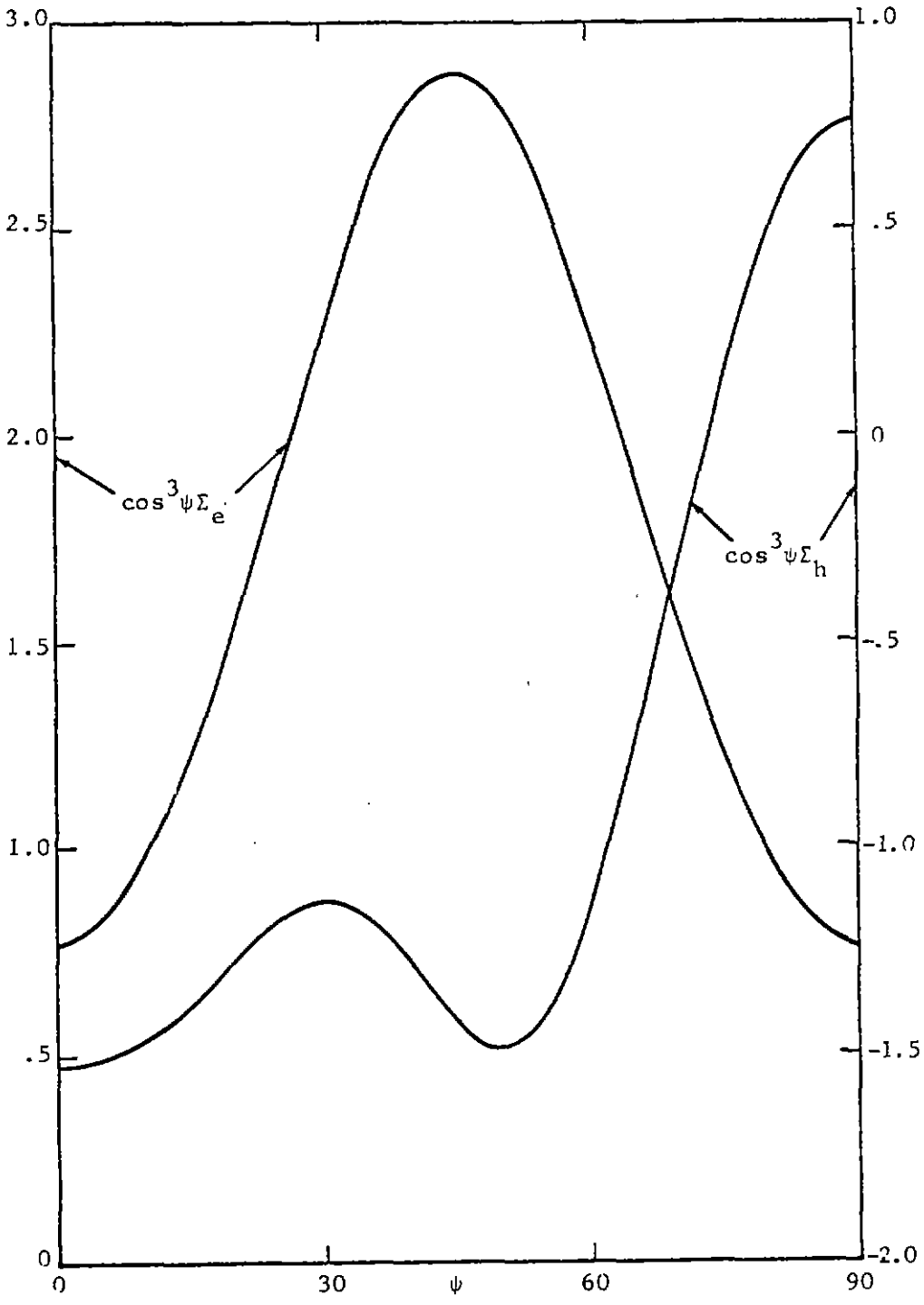

Figure 17. Auxiliary functions of interaction sums.

X. Another Look at the Braided Shield Model

Now that we have looked at some of the factors that influence the polarizabilities of small holes, we can continue the discussion begun in Section V, and arrive at some quantitative estimates of the shielding parameters of braided shields. Before we do this, however, it might be helpful to mention explicitly some of the effects that are not taken into account by the braided shield model of this note. This is done so that the reader can have a better basis for judging the overall accuracy and usefulness of the numerical data to follow.

Seven kinds of effects that are not taken into account by the present braided shield model, in approximate order of increasing difficulty with which they may be incorporated into the model, are:

1. Interior dielectric effects

   If there is a dielectric insulator between the inner conducting cable and the braided shield, the formulas developed in Section III would require slight and obvious revisions. In addition, it is simple to show that the electric polarizability of a hole, calculated by the method of Section VI, should be multiplied by $2(1 + \varepsilon_r)^{-1}$, where ε_r is the relative permittivity of the interior dielectric. All in all, this is a very simple effect to take into account; we have not done so in this note, mainly in an attempt to simplify and condense the material presented.

2. Exterior dielectric effects

   If the shielded cable is embedded in a conducting dielectric there will, of course, be further complications in several of the formulas of this note.

3. Effect of shield curvature on hole interaction

   The interaction sums we have computed in the previous section were over a planar array of holes. If the transverse hole spacing of the braid is not small compared to the shield diameter, it may be necessary to take account of the actual shape of the cylindrical surface in which the holes are located. This would present no great numerical difficulty, but it would introduce an additional parameter into the study — the ratio of the transverse hole spacing to the

shield's radius of curvature near the position of the hole. We have tried, in this note, to keep the number of parameters to a minimum.

4. First order shield thickness effect

The finite thickness of the braid, which is neglected in the present model, may be partially taken into account by modifying the hole polarizability calculation. It would not be much more trouble, numerically, to modify the procedure of Section VI to calculate the polarizabilities of a hole in an infinite plate of finite thickness. One formulation of such a calculation would be to derive coupled integral equations for the potentials (or their derivatives) over the surfaces defined by the intersections of the top and bottom of the plate with the cylinder defining the hole. This formulation could be carried out for those hole shapes for which the Green's function for the interior region of the hole (the region within the hole and between the top and bottom plane surfaces of the plate) is known. Elliptical and rectangular holes are examples of such hole shapes. There is, of course, in addition to this simple kind of modification of hole polarizabilities, a more complex shield thickness effect involving the peculiar woven fabrication of the braid; we will discuss this as effect (6), below.

5. Shield conductivity effects

The effect of shield conductivity may be taken into account, to first order, by adding another term to the transmission-line equation (5.1). Such terms have been discussed in references [1] and [2], for example. At low frequency this source term reduces to $(I_T - I)R$, where R is the d.c. resistance per unit length of the shield. The finite resistance of the shield wires would also have an effect on the L_s and S_s parameters that we have discussed in the present note. The understanding and calculation of the modification of L_s and S_s by the presence of resistance should be the subject of a future study.

6. Braid weave effects

The particular construction of braided shields gives rise to effects depending on the thickness of the braid wires that are distinct from the first order thickness effect discussed as number (4) above.

What we have in mind is that, because of the woven fabrication of the braid, the holes between braid bands are actually larger than they appear when looking at a sheet of the braid material along a normal to the sheet. Thus, a braid with "95%" optical coverage can have the sum of its hole areas make up more than 5% of the surface of the braid, if one looks at each hole in the direction from which it looks its largest. The algebra to go with these elementary observations is not at all elementary, and is beyond the scope of the present note.

7. Imperfect contact effects

If the wires of the braid have imperfect or irregular surfaces, so that there is some impedance between the individual wires, the model that we have developed will not be applicable without some modification. One form this modification might take would involve the sheet impedance concept; the shield surface in which the holes are located would be allowed to have a sheet impedance. This could partially account for the tendency of current to flow along the direction of the wires, rather than between the wires, if the wire surfaces are in imperfect contact. A more precise statement and treatment of the imperfect contact problem must be left to future work.

Now let us return to our object of obtaining some numerical estimates of the shielding parameters of a braided shield. Referring to Section V, the parameters of particular interest, L_s and S_s, are given by equations (5.22) and (5.24). For convenience, we repeat these formulas here.

$$L_s = -\frac{\mu_o w}{P}\frac{(1-c)^{3/2}}{1-(1-c)^{1/2}}\bar{\alpha}_m(\psi)\langle d_i d_e\rangle \tag{10.1}$$

$$S_s = -\frac{w}{\varepsilon_o P}\frac{(1-c)^{3/2}}{1-(1-c)^{1/2}}\bar{\alpha}_e(\psi)\langle d_i d_e\rangle \tag{10.2}$$

We wish to study, in particular, the variation of these parameters with the weave angle of the braid, the optical coverage of the braid being kept constant. With this in mind let us rewrite the above equations as

$$L_s = L_s^o \overline{\alpha}_m(\psi)$$

and

$$S_s = S_s^o \overline{\alpha}_e(\psi)$$

where the definitions of L_s^o and S_s^o are obvious. These quantities, L_s^o and S_s^o, are almost independent of the weave angle (there is a slight and unimportant dependence of the averaged density functions on the weave angle; we will forget about this), and so the quantities we are interested in calculating are just $\overline{\alpha}_m(\psi)$ and $\overline{\alpha}_e(\psi)$. From the discussion in Section V it is clear that these polarizabilities are the ratios between effective dipole moments and external field, the type of thing discussed in the previous section, and so a more informative notation might be

$$L_s = L_s^o \overline{\hat{\alpha}}_m(\psi) \tag{10.3}$$

$$S_s = S_s^o \overline{\hat{\alpha}}_e(\psi) \tag{10.4}$$

Of the four factors we have examined that influence the values of the polarizabilities, it can be seen, from the previous four sections, that the most important, for most of the cases we are interested in, are the effects of hole shape and hole-hole interactions. Taking account of only these two effects, the quantities of interest may be written as

$$\overline{\hat{\alpha}}_m(\psi) = \frac{P_h}{A^2} \frac{\alpha_m}{1+(\alpha_m/w_x^2)\Sigma_h}$$

$$= \frac{\overline{\alpha}_m(\psi)}{1+(A^2/P_h)(\overline{\alpha}_m(\psi)/w_x^2)\Sigma_h} \tag{10.5}$$

and

$$\overline{\hat{\alpha}}_e(\psi) = \frac{P_h}{A^2} \frac{\alpha_e}{1+(\alpha_e/w_x^2)\Sigma_e}$$

$$= \frac{\overline{\alpha}_e(\psi)}{1+(A^2/P_h)(\overline{\alpha}_e(\psi)/w_x^2)\Sigma_e} \tag{10.6}$$

where $\bar{\alpha}_m(\psi)$ and $\bar{\alpha}_e(\psi)$ are the normalized polarizabilities calculated by the method of Section VI, and Σ_h and Σ_e are the interactions sums calculated in Section IX. It is not difficult to show, for diamond-shaped holes in a diamond lattice representing a braid of optical coverage c and weave angle ψ, equations (10.5) and (10.6) reduce to

$$\bar{\hat{\alpha}}_m(\psi) = \bar{\alpha}_m(\psi)\left\{1 + \frac{(1-c)^{3/2}\,\bar{\alpha}_m(\psi)\cos^3\psi}{4\sin 2\psi}\,\Sigma_h\right\}^{-1} \tag{10.7}$$

and

$$\bar{\hat{\alpha}}_e(\psi) = \bar{\alpha}_e(\psi)\left\{1 + \frac{(1-c)^{3/2}\,\bar{\alpha}_e(\psi)\cos^3\psi}{4\sin 2\psi}\,\Sigma_e\right\}^{-1} \tag{10.8}$$

The above expressions have been evaluated numerically by employing tables 1b, 2b, and 5. The results of this evaluation, for values of ψ given by $5^\circ(5^\circ)45^\circ$, are presented in table 6 and figure 18, for various values of c. Because of the approximate nature of equations (10.7) and (10.8), we have presented only two significant figures in the table.

From the table and curves we see that our approximation to $\bar{\hat{\alpha}}_m(\psi)$, the normalized value of L_s, has a minimum as a function of ψ which, for most values of c, occurs between 10° and 20°. A minimum in this quantity has also been observed experimentally. We have not extended our table to values of ψ higher than 45°, since these values are not very interesting. We note that, for higher values of c, the value of ψ at which the minimum occurs gets smaller. But we must always keep in mind effect (6) of this section; the higher values of c give rise to bigger holes than would be predicted by a geometrical optical coverage argument. It is believed that, if this effect could be properly taken into account, the position of the minimum would be more insensitive to c.

We also note from the tables and curves that $\bar{\hat{\alpha}}_e(\psi)$ has a slight maximum, as a function of ψ, again for ψ somewhere between 10° and 20°. It would be interesting to have some experimental data on this quantity.

Table 6

Effect of weave angle on normalized shielding parameters

a. $\bar{\hat{\alpha}}_m(\psi)$

ψ \ c	0	.1	.2	.3	.4	.5	.6	.7	.8	.9
5		51.60	3.12	1.66	1.15	.90	.75	.66	.59	.55
10	1.34	1.11	.95	.84	.76	.70	.65	.61	.58	.56
15	.97	.88	.81	.76	.71	.68	.65	.62	.60	.59
20	.89	.84	.79	.75	.72	.69	.67	.65	.64	.63
25	.89	.85	.81	.78	.75	.73	.71	.69	.68	.67
30	.95	.91	.87	.84	.81	.79	.77	.75	.74	.73
35	1.07	1.02	.98	.94	.91	.88	.86	.84	.82	.81
40	1.29	1.21	1.15	1.10	1.05	1.01	.98	.95	.93	.92
45	1.65	1.52	1.42	1.33	1.20	1.10	1.15	1.11	1.08	1.05

b. $\bar{\hat{\alpha}}_e(\psi)$

ψ \ c	0	.1	.2	.3	.4	.5	.6	.7	.8	.9
5	.37	.39	.40	.42	.44	.45	.47	.48	.50	.51
10	.43	.44	.44	.46	.46	.47	.48	.49	.50	.50
15	.44	.45	.45	.46	.47	.47	.48	.48	.49	.49
20	.44	.45	.45	.46	.46	.47	.47	.47	.48	.48
25	.44	.44	.45	.45	.46	.46	.46	.47	.47	.47
30	.44	.44	.44	.45	.45	.45	.46	.46	.46	.46
35	.43	.44	.44	.44	.45	.45	.45	.45	.46	.46
40	.43	.44	.44	.44	.45	.45	.45	.45	.45	.46
45	.43	.44	.44	.44	.44	.45	.45	.45	.45	.45

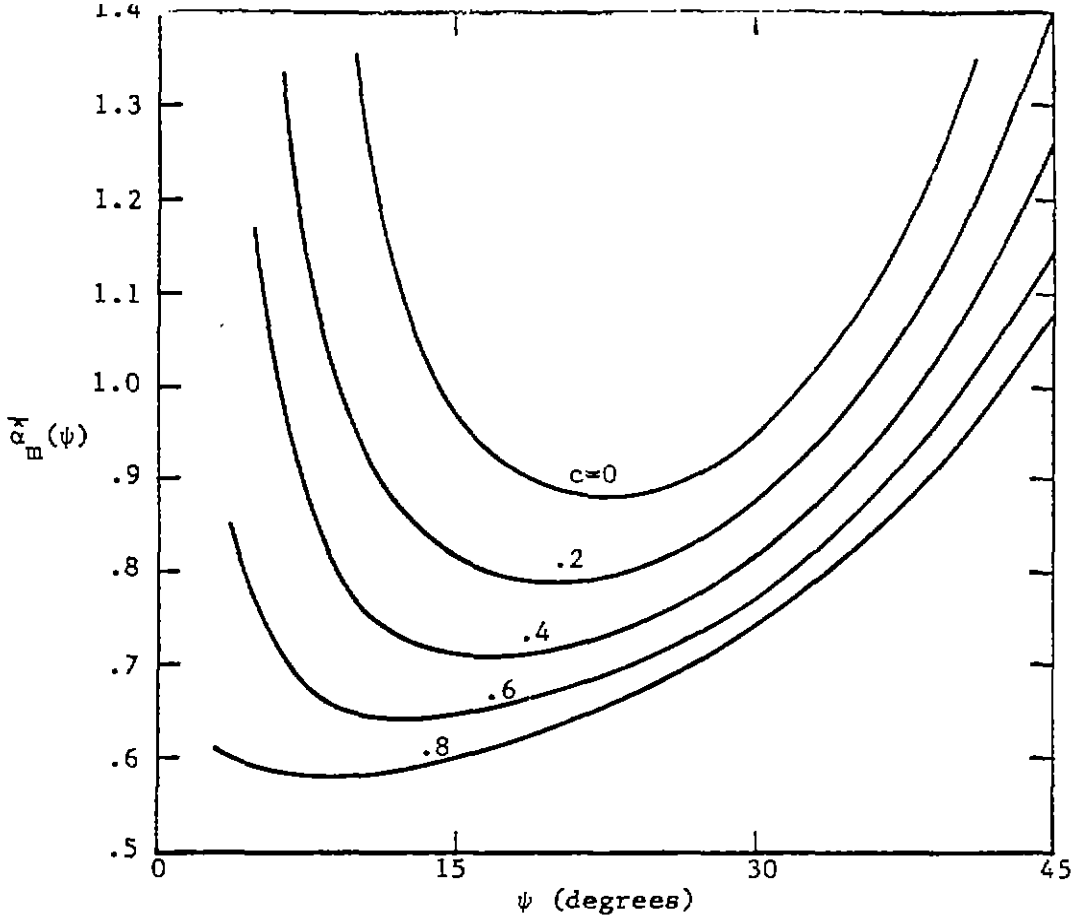

Figure 18a. Normalized L_s as a function of ψ.

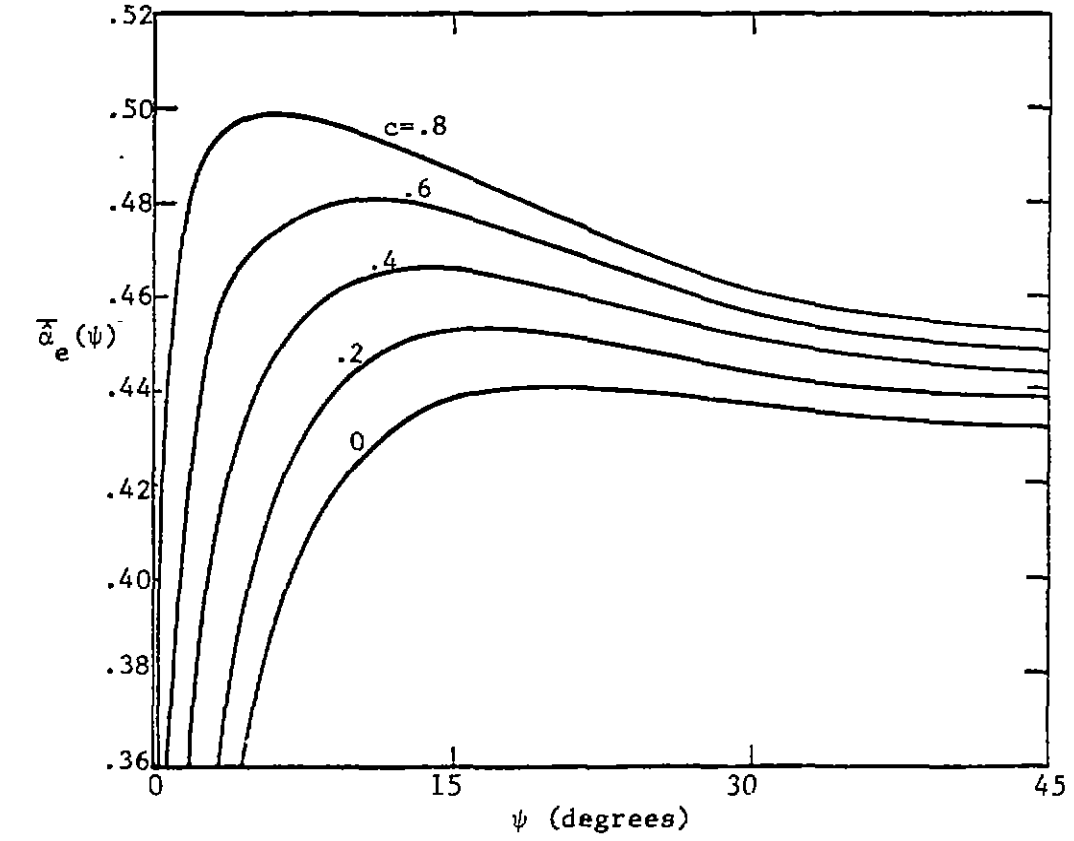

Figure 18b. Normalized S_s as a function of ψ.

References

[1] E. F. Vance and H. Chang, "Shielding effectiveness of braided wire shields," to be published as an EMP Interaction Note.

[2] H. Kalen, Wirbelströme und Schirmung in der Nachrichtentechnik, Springer-Verlag, Berlin, 1959.

[3] R. W. Latham, "An approach to certain cable shielding calculations," Interaction Note 90, January, 1972.

[4] Clayborne D. Taylor and Charles W. Harrison, Jr., "On the excitation of a coaxial line through a small aperture in the outer sheath," Interaction Note 104, January, 1972.

[5] William R. Smythe, Static and Dynamic Electricity, McGraw-Hill, New York, 1950.

[6] J. J. Bowman, T. B. A. Senior and P. L. E. Uslenghi, editors, Electromagnetic and Acoustic Scattering by Simple Shapes, North-Holland, Amsterdam, 1969.

[7] Philip M. Morse and Herman Feshbach, Methods of Theoretical Physics, McGraw-Hill, New York, 1953.

[8] Milton Abromowitz and Irene A. Stegun, editors, Handbook of Mathematical Functions, National Bureau of Standards, AMS-55, 1964.

[9] Ian N. Sneddon, Mixed Boundary Value Problems in Potential Theory, North-Holland, Amsterdam, 1966.